# Generative Pattern Dissemination for Collaborative Intrusion Detection

A thesis presented for the degree of Master of Science
by Mike Petersen

First Reviewer: Prof. Dr. Ulrich Bühler
Second Reviewer: Prof. Dr. Sebastian Rieger

Department of Computer Sciences
University of Applied Sciences Fulda
Fulda, Germany
July 2021

# Abstract

# Contents

# Chapter 1

# Introduction

## 1.1 Motivation

## 1.2 Objectives

## 1.3 Structure

# Chapter 2

# Preliminaries

## 2.1 Intrusion Detection

This section introduces the topic of intrusion detection and some important subcategories in the context of the thesis. First, IDSs are described and categorized according to different characteristics. The advantages and disadvantages of individual types of IDS are explained and examples are referred to individually. The topic of network flow monitoring is then addressed, since it is an essential component of network monitoring that is incorporated in the proposed architecture. The role of network flows in the context of network management is motivated and the typical processes of a flow exporter are described. In the context of the shortcomings of conventional IDSs for protecting large scale systems against coordinated and distributed attacks, Collaborative Intrusion Detection Systems (CIDSs) are introduced. For this purpose, it is first described what coordinated and distributed attacks are. Then it is explained what constitutes CIDS, what requirements exist for the realization of CIDS, and what components and processes CIDS typically consist of.

### 2.1.1 Intrusion Detection Systems

Classic security mechanisms, such as encryption or firewalls, are considered as preventive measures for protecting IT infrastructures. However, in order to be able to react to security breaches that have already occurred, additional reactive mechanisms are required. To complement preventive measures, Intrusion Detection Systems (IDSs) have been commercially available since the late 1990s [WM18, p. 27]. Generally, the main reason for operating an IDS is to monitor and analyze computer networks or systems in order to identify anomalies, intrusions or privacy violations [Hin+20]. Specifically, the following three advantages are significant [WM18, p. 391].

- IDSs can detect the preliminaries of attacks, in particular the organized gathering of information about networks and defense mechanisms (attack reconnaissance), and thus enable the prevention or mitigation of damage to information assets.
- IDSs can help protect information assets when known vulnerabilities cannot be fixed fast enough, notably in the context of an rapidly changing threat environment.
- The occurrence of unknown security vulnerabilities (zero day vulnerabilities) is not predictable, meaning that no specific preparations can be made for them. However, IDSs can identify processes in the IT system that deviate from the normal state and thus contribute to the detection of zero day attacks

For an effective IDS, it is important to be able to detect as many steps as possible within the prototypical attack sequence, also called kill chain [WM18, p. 393]. Since a successful intrusion into a system can be stopped at several points in this sequence, the effectiveness of the IDS increases with its functionality. The following categorization (see Figure 2.1) of intrusion attempts according to [Ken99] reflects parts of that chain.

*Probing* refers to the preambles of actual attacks, also known as attack reconnaissance. This includes obtaining information about an organization and its network behavior (footprinting) and obtaining detailed information about the used operating systems, network protocols or hardware devices (fingerprinting).

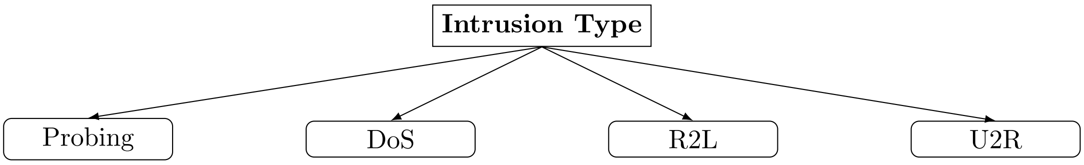

Figure 2.1: A categorization of intrusions into different subtypes

*Denial of Service* (DoS) refers to an attack aimed at disabling a particular service for legitimate users by overloading the target systems processing capacity. *Remote to Local* (R2L) attacks attempt to gain local access to the target system via a network connection. And one step further, *User to Root* (U2R) attacks start out with user access on the system and gain root access by exploiting vulnerabilities. Individual intrusion types can but do not have to be executed consecutively. For example, it is not mandatory to render a system incapable of action by DoS in order to subsequently gain local access to the target. However, this may be part of a strategy.

Additionally, IDS are generally categorized by the detection scope and the employed attack detection method [Mil+15]. Hence, a distinction is made between Host-based Intrusion Detection System (HIDS) and Network-based Intrusion Detection System (NIDS). While a HIDS resides on a system, known as host, only monitoring local activities, a NIDS resides on a network segment and monitors remote attacks that are carried out across the segment. In general, HIDS are advantageous if individual hosts are to be monitored. NIDS, on the other hand, are able to monitor traffic coming in and out of several hosts simultaneously. The disadvantage of NIDS, however, is that attacks can only be detected if they are also reflected in the network traffic. Pioneering examples in the context of HIDS are the Intrusion-Detection Expert System (IDES) [LTG92] and the Multics Intrusion Detection and Alerting System (MIDAS) [Seb+88]. A prominent representative in the area of NIDS is NetSTAT [VK98] [VK99].

Furthermore, IDS are categorized into misuse-based detection and anomaly-based detection (see Figure 2.2). A misuse-based approach defines a model that describes intrusive behaviour and compares the system or network state against that model. An anomaly-based IDS, on the other hand, creates a statistical baseline profile of the system's or network's normal state and compares it with monitored activities. The concept of the NIDS origins from [Den87].

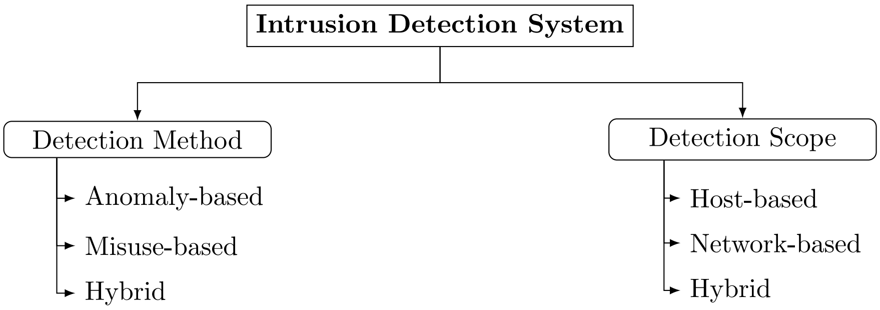

Figure 2.2: A taxonomy for IDS that distincts systems based on the utilized detection method or the scope in which it operates

Obviously, these two opposing approaches offer different advantages and disadvantages and are capable of complementing each other. Misuse-based systems can detect malicious behavior with a low false positive rate, but assume that the exact patterns are known. Typically, this method cannot detect novel [WM18, p. 403], metamorphic or polymorphic attacks [Szo05, p. 236]. An anomaly-based approach allows both known and unknown attacks to be detected, but the frequent occurrence of false-positive estimations is a major challenge. Given the amount of data that occurs in computer systems and networks nowadays, the generation of false alarms for even a fraction of this amount can render the IDS operationally unusable, since no network administrator can investigate such a large number of incidents in detail [Axe00]. Most implementations of misuse-based systems rely on the creation of signatures. A signature is similar to a collection of rules that describes an attack pattern. The most prominent signature-based IDS is Snort [Roe+99]. The payload-based anomaly detector PAYL [WS04] is an example for an anomaly-based system. Hybrid approaches are conceivable in order to circumvent the respective disadvantages of different subcategories of IDS. The interested reader is referred to the following works [Dep+05] [ZZ06] [Bee21].

### 2.1.2 Network Flow Monitoring

Network monitoring is a key component for network management as network administrator derive decisions based on data that results from monitoring activities. By collecting data from network devices, such as switches, routers or clients, the current behaviour of the network is measured. Commonly, this behaviour has to meet some minimum application requirements, which can be summarized by the term Quality of Service (QoS) [TFW21, p. 406]. In this context, the most early and vague definition of a network flow was introduced as "a sequence of packets traveling from the source to the destination" [Cla88]. Here, no further characteristics of a flow are given and it is not clear how one flow is differentiated from another flow. Later in the 1990s, however, the demand arose for a finer-grained view of network traffic than that provided by interface-level counters, but without the disadvantage of the huge amounts of data generated by packet tracking. Evidently, the concept of network flows has filled this gap in demand and has gained a central role in network management and research today [TB11].

Since the first attempts at standardization in the 1990s through the efforts of the Internet Enginnering Task Force (IETF), a number of proprietary standards have emerged as each network device vendor has implemented its own flow export protocol. In order to improve interoperability in the area of network flow measurement, the IETF established the IP Flow Information Export (IPFIX) working group. This working group defined the IPFIX standard (RFC 5101), which defines the term network flow as follows.

A network flow is an aggregation of all network packets that pass an observation point of a network during a certain time interval and share a set of common properties. These properties are defined as the result of applying a function to the value of

1. one or more packet, transport or application header fields,
2. one ore more characteristics of the packet itself,
3. one or more fields derived from packet treatment.

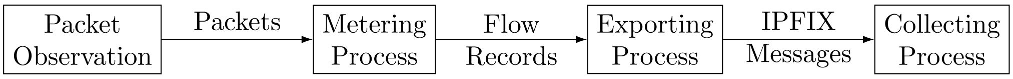

Figure 2.3: test

This definition is loose enough to cover the range from a flow containing all packets observed at a network interface to a flow that consists only of a single packet between two applications. Note, that this definition of the set of properties is also less strict than the conventional definition of the five-tuple consisting of source IP address, source port, destination IP address, destination port and protocol [Cla08]

In general, network flows can appear either as unidirectional flow, which aggregates all packets from host A to host B (or vice versa), or as bidirectional format, that aggregates all packets regardless of direction. Depending on which flow format and flow exporter is used, additional information, e.g. statistical calculations on bytes per second, can be obtained. Other common network flow protocols are NetFlow [Cla04], OpenFlow [McK+08] and sFlow [Pha].

Systems that generate flow data and extract additional information are called flow exporters. Generally, flow exporters are part of a general flow monitoring architecture [Hof+14], that consists of four different processes (see Figure 2.3). The *packet observation* is done on interfaces of packet forwarding devices by capturing network packets and executing specific preprocessing steps like timestamping and truncation. The process of *flow metering* describes the aggregation of packets into flow records. There, a set of functions, including packet header capturing, timestamping, sampling and classifying is applied on values of the packet stream listed above. Furthermore, flow records are maintained, which may include creating, deleting or udpating records, or computing statistical flow features. After that, Fthe *exporting process* places flow records in a datagram of the deployed export protocol and sends them to one or more collecting processes. Finally, the *collection process* is responsible for the reception, storage and preprocessing of flow records, produced by the preceding step. Typically, the collected data is analyzed. This can be done, for example, in the context of Intrusion Detection System (IDS) or traffic profiling.

Using network flows for intrusion detection has several advantages over Deep Packet Inspection (DPI). For example, DPI requires highly complex and expensive infrastructure for storage and analysis of the data [Hof+14]. Since flow exporter setups rely on packet header fields and statistical aggregations, a significant data reduction is achieved, which is why an analysis of network flows is scalable and also applicable for high-speed networks [Hof+14]. In addition, discarding the payload results in a better compliance with data retention laws and privacy policies.

### 2.1.3 Collaborative Intrusion Detection

attackers use automation to target all vulnerable services at once instead of manually targeting services [Sav05]

by using computing resources available through botnets or by simply renting instances on cloud vendors

large-scale coordinated attacks can be executed, which target a large number of hosts

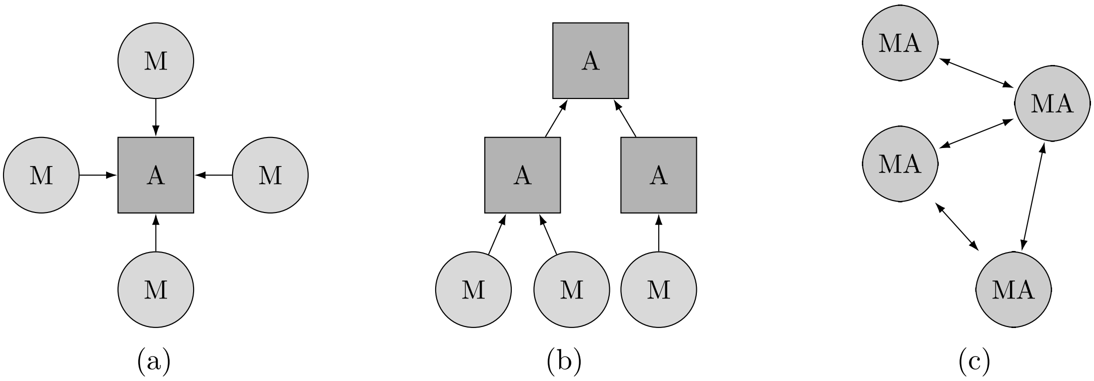

Figure 2.4: Bivariate gaussian distributions exhibit different shapes with a changing correlation value between the random variables $x_1$ and $x_2$: (a) negative, (b) zero and (c) positive correlation

which are spread over a wide geographical area [ZLK10]

examples are distributed scans, worm outbreaks and distributed DoS attacks.

According to [ZLK10], these attacks are difficult to detect by isolated IDS, because of their limited monitornig scope

Indeed, in [RGH12] it is shown that a distributed portscan can be executed with relatively few resources without being detected when deploying Snort IDS and a commercial firewall solution.

in order to detect such attacks, evidence of attacks from multiple different sources, i.e., infrastructures have to be combined, leading to the idea of collaborating intrusion detection systems (CIDS).

auch in bezug auf neuartige angriffe, wie bspw. zero days, sind CIDS ein Lösungsansatz, da Informationen über neuartige Angriffe mit anderen Mitgliedern im CIDS verbund geteilt werden

Zusätzlich zum Aspekt der verbesserten Detektion zeigen sich noch weitere Vorteile, wie bspw. die bessere Skalierung in großen IT Systemen; einzelne IDS können bei der Detektion großer Datenmengen zum Bottleneck werden. Bei Verwendung Mehrerer IDS im Verbund kann die Last verteilt werden und zur Resilienz des Systems in Bezug zur Verfügbarkeit erhöhen.

In general, a CIDS is a network of several intrusion detection components that collect and exchange data on system security. A CIDS is essentially specified by two different types of components, namely the detection units and the correlation units, and their communication among each other. The detections units can be considered as conventional IDS that monitor a sub-network or a host and by that, generate low-level intrusion alerts. The correlation unit is responsible for merging the low-level intrusion alerts and their further post-processing. This includes, for instance, the correlation of the alerts, the generation of reports or the distribution of the information to the participants of the network. CIDSs pursue the following two goals [Vas16, p. 24].

- The aggregation and correlation of data originating from different IDSs creates a holistic picture of the network to be monitored and enables the detection of distributed and coordinated attacks.

- CIDSs can monitor large-scale networks more effectively with the realization of a loadbalancing strategy. By sharing IDS resources across different infrastructures, short-term peak loads can be served, reducing the downtime of individual IDSs.

The requirements and key components are adopted from [**vas_2015**], who have summarized them within an survey. It should be noted that the structuring partly overlaps and that individual or several requirements influence each other.

### Requirements

**Accuracy** Accuracy generally describes a collection of evaluation metrics for assessing the performance of the Collaborative Intrusion Detection System (CIDS). Frequently used metrics are, for example, the Detection Rate (DR), i.e. the ratio of correctly detected attacks to the total number of attacks, or the False Postive Rate (FPR), which sets the number of normal data classified as an attack in relation to the total number of normal data.

**Minimal Overhead and Scalability** This requirement describes the operational overhead and the scalability of the system directly related to this. First, the algorithms and techniques for collecting, correlating, and aggregating data must require minimal computational overhead. Second, data distribution within the CIDS must be as efficient. The performance required to operate the system should increase linearly with the resources used, so that computer systems of any size can be protected by the CIDS. This property can be measured in theoretical terms by considering the complexity of the algorithms used. In practical terms, the passed time from the collection of a data point to the decision-making process can be measured.

**Resilience** Resilience describes the ability of the system to be resistant to attacks, manipulations and system failures. A distinction is made between external attacks, such as DoS, and internal attacks by infiltrated CIDS components. Moreover, it also covers fail-safety in general, which can be achieved, for example, by avoiding SPoFs.

**Privacy** With regard to the protection and regulation of communication in the CIDS, a distinction is made between internal and external communication. Data that is exchanged internally in the CIDS network between members may contain potentially sensitive information that should not be disclosed directly to other participants for reasons of data privacy.

This includes, among other things, legal aspects when it comes to sharing log and network data. In connection with the resilience of the system, securing communication against third parties using cryptographic methods also plays a role and represents a major challenge, especially in dynamically distributed architectures.

**Self-configuration** This requirement describes the degree of automation of a system with regard to configuration and operation. Particularly in distributed and complex architectures, a high degree of automation is desired in order to avoid operating errors and enable automatic resolution of component failures.

**Interoperability** The individual components of the overall system, which were deployed in different system and network environments, should be able to interact with each other in the context of the CIDS. In addition to system-wide standards for data collection, processing and exchange, there exists a trade-off between interoperability and privacy.

### Design Components

**Local Monitoring** First, a distinction is made between active and passive monitoring. Active monitoring refers to the use of honeypots that reveal themselves as attack targets in the infrastructure in order to collect attack data. Passive monitoring involves intrusion detection activity at the host or network level, which in turn can be divided into signature-based or anomaly-based methods according to the type of detection technique used (see Chapter **??**).

**Membership Management** Membership management refers to ensuring secure communication channels in the form of an overlay network. Generally, membership management is categorized according to the organization and structure of the system topology. In terms of organization, there are either static approaches, in which members are added or removed manually, or dynamic approaches, in which components are organized automatically via a central entity or a protocol. Furthermore, the structure of the overlay network is relevant for the type of communication in the CIDS network. This means that connections between the monitoring units are either centralized, hierarchical or distributed.

**Correlation and Aggregation** Before collected and analyzed data are shared with other participants in the CIDS network, the data is correlated and similar data points are aggregated. The main purpose of generating global and synthetic alerts is firstly to reduce the amount of alerts overall and secondly to improve data insights. Correlation mechanisms can be categorized into single-monitor and monitor-to-monitor approaches. Single-monitor methods correlate data locally without sharing data with other monitor entities. Monitor-to-monitor approaches, on the other hand, share data with other monitoring units in order to correlate local data with shared data and thus enable insights that go beyond isolated methods. Further, a classification can be made according to the correlation techniques used, grouping four different approaches.

- *Similarity-based* approaches correlate data based on the similarity of one or more attributes. For instance, [**goo_2001**] suggests using the 5-tuple information of the network data to detect duplicates within Network-based Intrusion Detection System (NIDS)s. The computation of similarity can be done in a variety of ways. For example, [**goo_2001b**] defines a similarity function for each attribute and computes the overall data similarity by combining the functions using an expectation of similarity. High-dimensional data is usually problematic, as the difficulty for an effective calculation of similarity increases with the number of attributes [**zho_2009**].
- *Attack scenario-based* approaches detect complex attacks based on databases that provide patterns for attack scenarios (e.g. [**hut_2004**], [**jaj_2002**]). Such approaches have high accuracy for already known attacks. However, the accuracy

decreases as soon as the patterns in the real data deviate from those in the database, since the definition of the scenario-rules are of a static quality in these approaches.

- *Multistage alert correlation* aims to detect unknown multistage attacks by correlating defined pre- and post-conditions of individual alerts (e.g. [**cup_2002**], [**che_2003**]). The idea behind the approach is based on the assumption that an attack is executed in preparation for a next step. The system states before and after an alert are modeled as pre- and postconditions, which are correlated with each other. While these approaches are more flexible than the all-static definition of attack scenarios, they still require the prior modeling of pre- and postconditions, which are based on expert knowledge.

- *Filter-based* approaches filter irrelevant data in order to reduce the number of alerts within the intrusion detection context. For example, [**goo_2002**] filters alerts by a ranking based on priorities of incidents. Priorities are calculated through comparing the target's known topology with the vulnerability requirements of the incident type. The rank that each alert is assigned to provides the probability for its validity. The accuracy of the filters is based on the quality of the description of the topology to be protected and require reconfiguration when changes are made to the infrastructure.

**Data Dissemination** Data Dissemination describes the efficient distribution of correlated and aggregated data in the CIDS network. How the data is disseminated is strongly influenced by the topology and membership management of the system. Centralized topologies have a predefined flow of information from the monitoring units to the central analysis unit. If the system is organized hierarchically, information flows statically or dynamically organized from lower monitoring units in the hierarchy to higher units. Distributed topologies allow the use of versatile strategies, such as flooding, selective flooding or publish-subscribe methods.

**Global Monitoring** Global monitoring mechanisms are needed for the detection of distributed attacks which isolated IDSs cannot detect due to the limited information base. Thus, the detection of distributed attacks relies on the insight obtained by combining data from different infrastructures. This means that global monitoring is strongly dependent on the employed correlation and aggregation techniques. The overall strategy of the CIDS is described by global monitoring and can have both generic and specific objectives.

## 2.2 Locality Sensitive Hashing

Finding similar objects, formally known as the nearest-neighbour search problem, is a central problem in computer science in general. And besides the exact search, it is also an important topic in the field of intrusion detection. For example, exact searches allow to compare the signatures of known malware with low false positive rates. Considering polymorphic attacks, however, it is essential to also detect all objects that are similar to the known attack and thus detect modified forms of it. In this context, this section presents a well-studied approach called *Locality Sensitive Hashing* (LSH) that solves an approximate version of the nearest-neighbour search problem by partitioning the search space with a hash function. This way, the searching problem is reduced to pairs that are most likely to be similar. Besides the application for solving the NN search problem, for which LSH was originally conceived, the concept has been proven to be effective for numerous other use cases, such as dimensionality reduction, clustering or classification. As the proposed generative pattern database integrates a locality-sensitive hash function for enabling both similarity search and data parallelism, LSH and a specific variant called *Random Projection* (RP) is described in detail in this section.

Section 2.2.1 introduces the approximate version of the nearest neighbour search problem as it is a prerequisite for the general definition of LSH. After that, Section 2.2.2 begins by clarifying the core idea of LSH and subsequently explains how to construct a locality-sensitive hash function. Lastly, a specific family of LSH that uses the cosine distance for similarity calculations, also known as *Random Projection* is presented in Section 2.2.3.

### 2.2.1 The Approximate Nearest Neigbour Problem

For general definitions of the nearest-neighbour search problem (NN) and its variants, a set of points $\mathcal{P} = \{\boldsymbol{p}_1, \dots, \boldsymbol{p}_N\}, N \in \mathbb{N}$ in a metric space $(\mathcal{X}, d)$ with $\mathcal{P} \subset \mathcal{X}$ and where $d$ is a metric on $\mathcal{X}$, i.e., a function $d : \mathcal{X} \times \mathcal{X} \to \mathbb{R}$ is considered. It is assumed that $d$ is a proper metric, which means that it is

1. *symmetric*: $d(\boldsymbol{p}, \boldsymbol{q}) = d(\boldsymbol{q}, \boldsymbol{p})$,
2. *reflexive*: $d(\boldsymbol{p}, \boldsymbol{q}) \leq 0$, $d(\boldsymbol{p}, \boldsymbol{q}) = 0 \iff \boldsymbol{p} = \boldsymbol{q}$ and satisfies the
3. *triangle inequality*: $d(\boldsymbol{p}, \boldsymbol{q}) \leq d(\boldsymbol{p}, \boldsymbol{s}) + d(\boldsymbol{s}, \boldsymbol{q})$.

Then, the general NN is stated as follows [IM98].

**Definition 1** (Nearest-neighbour search problem)**.** Construct a data structure so as to efficiently answer the following query: Given any query point $\boldsymbol{q} \in \mathcal{X}$, find some point $\boldsymbol{p} \in \mathcal{P}$ such that

$$\min_{\boldsymbol{q} \in \mathcal{X}} d(\boldsymbol{p}, \boldsymbol{q}). \tag{2.1}$$

As the algorithms in the presented approach operate on vectors of statistical flow features (see Section 2.1.2), the input set for specific definitions is usually restricted to $\mathbb{R}^D, D \in \mathbb{N}$. Thus, a specific example of Definition 1 in the context of this work includes high-dimensional data in $\mathcal{P} \in \mathbb{R}^D$ with $D \gg 1$ and could define $d$ as, e.g., the euclidean distance. In this case, an exhaustive search would require a query time of $O(DN)$. Unfortunately, all exact algorithms that provide a better time complexity than an exhaustive search require $O(2^D)$ space [Rub18]. This tradeoff between time and space complexity is usually referred to as “curse of dimensionality” and can only be resolved by accepting approximate solutions. The $c$-approximate nearest-neighbour problem ($c$-ANN) is defined as follows [IM98].

**Definition 2** ($c$-Approximate nearest-neighbour search problem)**.** For any given query point $\boldsymbol{q} \in \mathcal{X}$ and some approximation factor $c > 1$, find some point $\boldsymbol{p} \in \mathcal{P}$ such that

$$d(\boldsymbol{p}, \boldsymbol{q}) < c \cdot \min_{\boldsymbol{s} \in P} d(\boldsymbol{s}, \boldsymbol{q}). \tag{2.2}$$

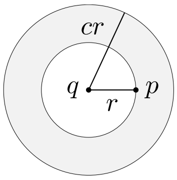

Figure 2.5: In the $cr$-approximate nearest-neighbour problem some point within $cr$ is accepted, if there exists a point $\boldsymbol{p}$ where $d(\boldsymbol{p},\boldsymbol{q}) \leq r$.

Thus, the distance from the query point $\boldsymbol{q}$ to the approximate nearest neighbour $\boldsymbol{p}$ is at most $c$ times the distance to the true nearest neighbour $\boldsymbol{s}$. However, LSH does not solve the $c$-ANN directly. Instead, the problem is relaxed first by introducing the $cr$-approximate nearest-neighbour problem ($cr$-ANN) as follows [IM98].

**Definition 3** ($cr$-Approximate nearest-neighbour search problem)**.** For any given query point $\boldsymbol{q} \in \mathcal{X}$, some approximation factor $c > 1$ and some target distance $r > 0$, if there exists a point $\boldsymbol{p} \in \mathcal{P}$ where $d(\boldsymbol{p},\boldsymbol{q}) \leq r$, then return a point $\boldsymbol{p}' \in \mathcal{P}$ where

$$d(\boldsymbol{p}',\boldsymbol{q}) \leq cr. \tag{2.3}$$

Figure 2.5 illustrates the $cr$-ANN. The target distance $r$ represents the distance of the query object from its nearest neighbour. If there is such a point, the algorithm returns points within $cr$ distance from the query object. Otherwise it returns nothing. It is shown that LSH can solve the $c$-ANN by solving the $cr$-ANN for different settings of $r$ [IM98].

### 2.2.2 Locality-Sensitive Hash Functions

Introduced by Indyck and Motwani in 1998 [IM98] as an algorithm that solves the $c$-ANN, locality-sensitive hashing (LSH) has since been extensively researched and is now considered among the state of the art for approximate searches in high-dimensional spaces.[1] The basic idea of the approach is to partition the input data using a hash function that is sensitive to the location of the input within the metric space. This way, similar inputs collide with a higher probability than inputs that are far apart. Thus, LSH exhibits fundamental differences to conventional hash functions.[2]

A hash function is a function that maps a large input set to a smaller target set. The elements of the input set are called *messages* or *keys* and may be of arbitrary different lengths. The elements of the target set are called *digests* or *hash values* and are of fixed size length. We define a conventional hash function as $h : \mathcal{M} \to \mathcal{B}$ where $\mathcal{M} \subset \mathcal{X}$ is the input set and $\mathcal{B} = \{0,1\}^K$ with $K \in \mathbb{N}$ the target set of all bit sequences of fixed size $K$, with $K < D$. It follows that messages $\boldsymbol{m} \in \mathcal{M}$ can only be mapped to $2^K$ different binary strings $\boldsymbol{b} \in \mathcal{B}$. The probability that a given $\boldsymbol{m}$ hashes to $\boldsymbol{b} = h(\boldsymbol{m})$ is $\frac{1}{K^2}$. Typically, conventional hashing is used for the realization of, e.g., hash tables, data integrity checks, error correction methods or database indexes. Such applications require a randomly uniform distribution of messages on hashes. Thus, a conventional hash function should therefore ideally assign hash values uniformly distributed with probability $\frac{1}{K^2}$ for all $\boldsymbol{m}$ and all $\boldsymbol{b}$. A related property in this context is the probability

[1] See [NBJ21] for an exhaustive survey of NN Techniques.

[2] Cryptographic and non-cryptograhpic hash functions are referred to as conventional hashing.

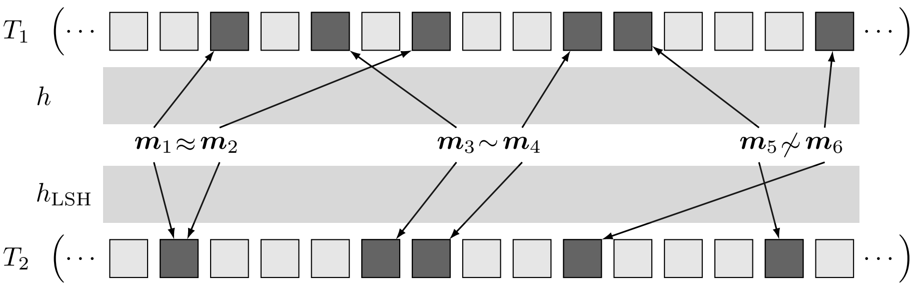

Figure 2.6: The behaviour of a conventional hashing function $h$ and a locality-sensitive hashing function $h_{\text{LSH}}$ when hashing very similar messages $\boldsymbol{m} \approx \boldsymbol{m}$, similar messages $\boldsymbol{m} \sim \boldsymbol{m}$ and non-similar messages $\boldsymbol{m} \not\sim \boldsymbol{m}$ into the slots of a hash table $T_1$ and $T_2$ respectively.

of a *collision*. A collision occurs when two messages $\boldsymbol{m}_1 \neq \boldsymbol{m}_2$ are projected onto the same hash value $h(\boldsymbol{m}_1) = h(\boldsymbol{m}_2)$. For example, cryptographic hash functions are used in systems, where adversaries try to break such systems. Thus, different security requirements are defined for cryptograhpic hash functions [Wil, p. 349]. In particular, these hash functions are designed to be resistant against collisions. Applications that do not require the hash function to be resistant against adversaries, e.g., hash tables, caches or de-duplication, are usually implemented by using a non-cryptographic hash function that exhibits relaxed guarantees on the security properties in exchange for significant performance improvements. However, both cryptographic and non-cryptographic hash functions behave relatively similar with respect to the distribution of messages on hashes and the probability of a collision. In contrast, locality-sensitive hash functions behave more or less inversely as illustrated in Figure 2.6. A conventional hashing function $h$ does not incorporate the similarity of messages into the calculation of the hash value. As a result, the messages are hashed evenly distributed into the slots of $T_1$. A locality-sensitive hashing function $h_{\text{LSH}}$ on the other hand, hashes more similar messages into the same slot or neighbouring slots of $T_2$ as the hashes reflect the similarity of the input messages. In this regard, the notation of a hash table is introduced. A hash table is defined as a tuple $T = (\boldsymbol{m}_{h(\boldsymbol{m})} \mid \boldsymbol{m} \in \mathcal{M})$ where $\mathcal{M}$ is the set of all messages that are selected to be stored in $T$. Thus, we simply say that a message $\boldsymbol{m}$ hashes to a slot $\boldsymbol{b} = h(\boldsymbol{m})$. Additionally, we define that the subset $h^{-1}(\boldsymbol{b})$ is made up of all the values associated with the key $\boldsymbol{b}$. Additionally, within an algorithm description the notation $T[\boldsymbol{b}]$ refers to the slot $\boldsymbol{b}$ of the hash table $T$, which enables a clearer expression for accessing nested hash table data structures.

As a locality-sensitive hashing function can be constructed as a general concept, specific families of functions can be derived. We refer to a *family* of hash functions $\mathcal{H} = \{h : \mathcal{M} \to \mathcal{B}\}$ as a collection of hash functions that have the same domain and range, share a basic structure and are only differentiated by constants. Three basic requirements are demanded for such a family of functions [LRU14, p. 99].

1. Close pairs of input should be hashed into the same bucket with higher probability than distant pairs.

2. Different functions within a family need to be statistically independent from one another, such that the FPR and FNR can be improved by combining two or more functions.

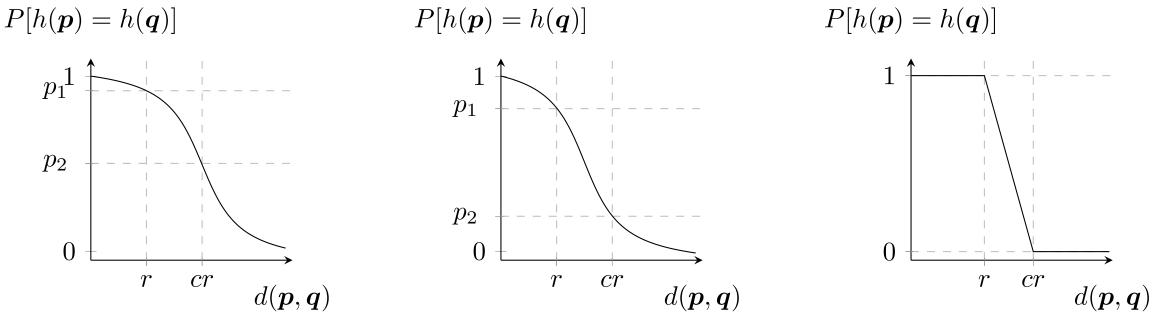

(a) Single LSH Function. (b) Amplified LSH Function. (c) Exact Search

Figure 2.7: The behaviour of a $(r, cr, p_1, p_2)$-sensitive function in (a) and (b) (adapted from [LRU14, p. 100]) approaching the ideal probability gap in (c) resembling the behaviour of an exact search.

3. Functions need to be efficient, i.e., be faster compared to an exhaustive search.

The first step is to define LSH generally. Applied on the $cr$-ANN, the first requirement states, with high probability, two points $\boldsymbol{p}, \boldsymbol{q}$ should hash to the same hash value if their distance is at most $r$, i.e., $d(\boldsymbol{p}, \boldsymbol{q}) \leq r$. And if their distance is at least $cr$, the points should hash to different hash values, i.e. $d(\boldsymbol{p}, \boldsymbol{q}) > cr$. Thus, A formal definition of a locality-sensitive hash function is given as follows [AI06].

**Definition 4** (Locality-Sesitive Hash Function)**.** Given a target distance $r \in \mathbb{R}, r > 0$, an approximation factor $c \in \mathbb{R}, c > 1$ and probability thresholds $p_1, p_2 \in \mathbb{R}$, a family $\mathcal{H} = \{h : \mathcal{P} \to \mathcal{B}\}$ is called $(r, cr, p_1, p_2)$-sensitive if for any two points $\boldsymbol{p} \in \mathcal{P} \subset \mathcal{X}, \boldsymbol{q} \in \mathcal{X}$ and any hash function $h$ chosen uniformly at random from $\mathcal{H}$ the following conditions are satisfied:

$$\begin{aligned} d(\boldsymbol{p}, \boldsymbol{q}) \leq r &\implies P[h(\boldsymbol{p}) = h(\boldsymbol{q})] \geq p_1, \\ d(\boldsymbol{p}, \boldsymbol{q}) \geq cr &\implies P[h(\boldsymbol{p}) = h(\boldsymbol{q})] \leq p_2. \end{aligned}$$

Ideally, the gap between $p_1$ and $p_2$ should be as big as possible as depicted in Figure 2.7c, which in fact represents an exact search. This is, as already discussed, no option due to its time and space requirements. Considering a single locality-sensitive function as shown in Figure 2.7a, where the probability gap between $p_1$ and $p_2$ is relatively close, the false negative rate would be relatively high. Increasing the gap would require to increase $c$ and lead to a high number of false positives. Therefore, a single function would provide only a tradeoff. But it is possible to increase $p_1$ close to 1 and decrease $p_2$ close to $1/N$ while keeping $r$ and $cr$ fixed as shown in Figure 2.7b by introducing a process called *amplification*. Two different forms, namely the AND-construction and the OR-construction, can be applied.

By applying a logical AND-construction on $\mathcal{H}$ the threshold $p_2$ is reduced. For that, $K$ hash functions are sampled indepedently from $\mathcal{H}$ and each point $\boldsymbol{p}$ is hashed to a $K$-dimensional vector with a new constructed function $g \in \mathcal{H}^K$ as

$$g(p) = [h_1(\boldsymbol{p}), h_2(\boldsymbol{p}), \ldots, h_K(\boldsymbol{p})]. \tag{2.4}$$

Since all hash functions $\{h_1, \ldots, h_K\} \in \mathcal{H}$ are statistically independent the product rule applies and for any two points $\boldsymbol{p}$ and $\boldsymbol{q}$, a collision occurs if and only if $h_k(\boldsymbol{p}) = h_k(\boldsymbol{q})$

for all $k \in \{1, \dots, K\}$. The probability gap is then defined as follows:

$$\begin{aligned} P[h_k(\boldsymbol{p}) = h_k(\boldsymbol{q})] \geq p_1 &\implies P[g(\boldsymbol{p}) = g(\boldsymbol{q})] \geq p_1^K \\ P[h_k(\boldsymbol{p}) = h_k(\boldsymbol{q})] \leq p_2 &\implies P[g(\boldsymbol{p}) = g(\boldsymbol{q})] \leq p_2^K. \end{aligned}$$

Thus, by increasing $K$ the threshold $p_2$ can be arbitrarily decreased and approaches zero. However, the AND-construction lowers both $p_1$ and $p_2$. In order to improve $p_1$, the OR-construction is introduced. For that, a number of $L \in \mathbb{N}$ functions $\{g_1, \dots, g_L\}$ are constructed, where each function $g_l$, $l \in \{1, \dots, L\}$ stems from a different family $\mathcal{H}_l$. Note, that the algorithm is successful, when the two points $\boldsymbol{p}, \boldsymbol{q}$ collide at least once for some $g_l$. Therefore, hashing a point $\boldsymbol{p}$ with each $g_l$ results in the following probability for collision.

$$\begin{aligned} P[\exists l, g_l(\boldsymbol{p}) = g_l(\boldsymbol{q})] &= 1 - P[\forall l, g_l(\boldsymbol{p}) \neq g_l(\boldsymbol{q})] \\ &= 1 - P[g_l(\boldsymbol{p}) \neq g_l(\boldsymbol{q})]^L \\ &\geq 1 - (1 - p_1^K)^L \end{aligned}$$

As the AND-construction lowers both $p_1$ and $p_2$, similarly the OR-construction rises both thresholds. By choosing $K$ and $L$ judiciously, $p_2$ approaches zero while $p_1$ approaches one. Both constructions may be concatenated in any order to manipulate $p_1$ and $p_2$. Of course, the more constructions are used and the higher the values for the parameters $K$ and $L$ are picked, the more time is considered for the application of the function.

The general algorithm for solving the $cr$-ANN using LSH consists of two consecutive steps. First, a set of points is required for the construction of the data structure as described in Algorithm 1. For each function $g_l$ a corresponding hash table $T_l$ is initialized that will store all data points $\boldsymbol{p}_n$. In other words, all data points are preprocessed and stored $L$ times.The resulting data structure represents the database, which is searched through, when answering a query. Note, that a common collision handling method, such as seperate chaining for example, is applied if a certain slot is already occupied.

```
Input: $N$ points $\boldsymbol{p}_n \in \mathcal{P}$ with $n \in \{1, \dots, N\}, N \in \mathbb{N}$
Output: data structure $\mathcal{T} = \{T_1, \dots, T_L\}$
$\mathcal{T} \leftarrow \emptyset$
construct hash functions $g_1, \dots, g_L$ each of length $K$ (see Equation 2.4)
for each $g_l \in \{g_1, \dots, g_L\}$ do
    $T_l \leftarrow$ new hash table
    for each $\boldsymbol{p}_n \in \mathcal{P}$ do
        $T_l[g_l(\boldsymbol{p}_n)] \leftarrow \boldsymbol{p}_n$
    add $T_l$ to $\mathcal{T}$
return $\mathcal{T}$
```

Algorithm 1: LSH Preprocessing

Answering a query point $\boldsymbol{q}$ is done by hashing it multiple times for each $g_l$ as in the preprocessing step (see Algorithm 2). Each time, the set of points $\mathcal{P}$, stored in the correspoding hash table $T_l$ at the slot $g_l(\boldsymbol{q})$, are retrieved. That is, identify all $\boldsymbol{p}_n$, such that $g_l(\boldsymbol{p}_n) = g_l(\boldsymbol{q})$. For each identified $\boldsymbol{p}_n$, a distance function evaluates if the distance $d(\boldsymbol{p}_n, \boldsymbol{q})$ is within the search perimeter $cr$. If positive, the point is added to the result set $\mathcal{S}$, which is returned at the end of the algorithm.

```
Input: a query point $\boldsymbol{q}$ and data structure $\mathcal{T} = \{T_1, \dots, T_L\}$
Output: a set $\mathcal{S}$ of nearest neighours of $\boldsymbol{q}$
$\mathcal{S} \leftarrow \emptyset$
for each $g_l \in \{g_1, \dots, g_L\}$ do
    $\mathcal{S}_l \leftarrow T_l[g_l(\boldsymbol{q})]$
    if $|\mathcal{S}_l| > 0$ then
        for each $\boldsymbol{p}_n \in \mathcal{S}_l$ do
            if $d(\boldsymbol{p}_n, \boldsymbol{q}) \leq cr$ then
                add $\boldsymbol{p}_n$ to $\mathcal{S}$
return $\mathcal{S}$
```

Algorithm 2: LSH Query

With regard to preprocessing, the consideration of space complexity of Algorithm 1 is interesting, whereas the runtime of Algorithm 2 is the most relevant when examining the execution of queries. Fortunately, lower bounds on both quantities have been proven in [MNP06], resulting in the following theorem.

**Theorem 5.** Let $(\mathcal{X}, d)$ be a metric on a subset of $\mathbb{R}^D$. Let be a $(r, cr, p_1, p_2)$-locality sensitive hash family $\mathcal{H}$ and write $\rho = \frac{\log(1/p_1)}{\log(1/p_2)}$. Then for $\mathcal{P} \subset \mathcal{X}$ and $N = |\mathcal{P}|$ and for any $N \geq \frac{1}{p_2}$ there exists a solution to $cr$-ANN with space complexity $O(DN + N^{1+\rho})$ and query time of $O(N^\rho)$.

Therefore, it follows that the query time of LSH can only be sublinear, if $\rho < 1$, which is the case if the inequality $p_1 > p_2$ is satisfied.

### 2.2.3 Random Projection

This section presents a specific technique that is a locality-sensitive hashing function. The algorithm that bases on this technique is known as Gaussian Random Projection (GRP). This approach utilizes the cosine similarity of two real vectors in order to determine their similarity. In the course of this section, basic definitions for Cosine Distance and Cosine Similarity are introduced. Then, the individual calculation steps of the approach are specified. Finally, a visual proof verifies that gaussian random projection (GRP) is a form of LSH.

The cosine distance can be applied in euclidean spaces and discrete versions of euclidean spaces [LRU14, p. 95]. For two real vectors $\boldsymbol{p}_1$ and $\boldsymbol{p}_2$, the cosine distance between is equal to the the angle between $\boldsymbol{p}_1$ and $\boldsymbol{p}_2$, regardless of the dimensionality of the space. Note, that by applying the arc-cosine function, the result is in the range $[0, 180]$. The following definition formalizes what has been stated so far.

**Definition 6** (Cosine Distance)**.** Given two vectors $\boldsymbol{p}_1$ and $\boldsymbol{p}_2$, the cosine distance $\theta(\boldsymbol{p}_1, \boldsymbol{p}_2)$ is the dot product of $\boldsymbol{p}_1$ and $\boldsymbol{p}_2$ divided by their euclidean distances from the

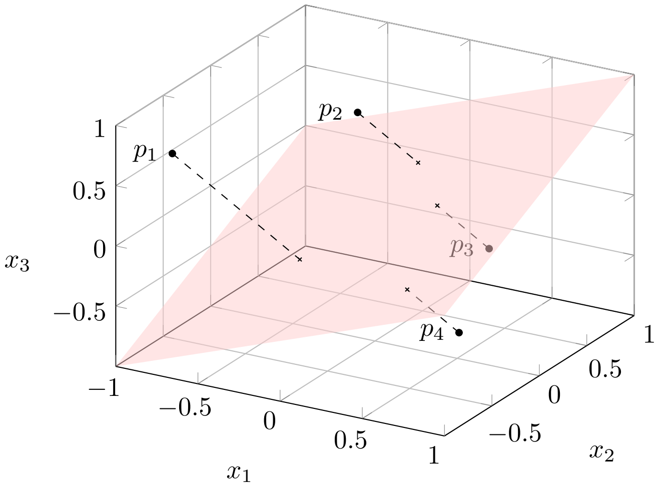

Figure 2.8: Illustration of a random hyperplane (red) partitioning the space

origin ($L_2$-norm):

$$\theta(\boldsymbol{p}_1, \boldsymbol{p}_2) = \cos^{-1}\left(\frac{\boldsymbol{p}_1^\top \boldsymbol{p}_2}{||\boldsymbol{p}_1||\ ||\boldsymbol{p}_2||}\right). \tag{2.5}$$

The angle $\theta$ can be normalized to the range $[0, 1]$ by dividing it by $\pi$. This way, the cosine similarity is simply given by the following definition.

**Definition 7** (Cosine Similarity)**.** The cosine similarity is computed as

$$1 - \frac{\theta(\boldsymbol{p}_1, \boldsymbol{p}_2)}{\pi} \tag{2.6}$$

Introduced in [Cha02], the GRP is defined as follows. Given a point $\boldsymbol{p} \in \mathcal{P} \subset \mathbb{R}^D$ and a randomly selected hyperplane defined as $\boldsymbol{M} = (a_{ij}) \in \mathbb{R}^{D \times K}$ where $a \sim \mathcal{N}(0, I)$, a *gaussian random projection (GRP)* aims to (I) reduce the dimensionality from $D$ to $K$ dimensions and (II) provide a binary encoding by first projecting $\boldsymbol{p}$ onto $\boldsymbol{M}$ and subsequently applying the sign function to each element of the result, which can be formalized as

$$h(\boldsymbol{p}) = [h(\boldsymbol{p}, a_1), \ldots, h(\boldsymbol{p}, a_k)] \text{ with } h(\boldsymbol{p}, a) = sign(\boldsymbol{p}^\top a) \tag{2.7}$$

$$\text{with } sign(x) = \begin{cases} 0 & \text{if } x < 0, \\ 1 & \text{if } x \geq 0. \end{cases} \tag{2.8}$$

An illistration of a random hyperplane that dissects the three-dimensional space and partitions the data space is given in Figure 2.8. The resulting digest is a binary vector $h(\boldsymbol{p}) = \boldsymbol{b} \in \mathcal{B}$ with $\mathcal{B} = \{0, 1\}^K$ that is used as bucket index for storing $\boldsymbol{p}$ in a hash table. For any two messages $\boldsymbol{p}_1, \boldsymbol{p}_2$, the probability of being hashed to the same bucket increases with a decreasing distance, given as

$$P[h(\boldsymbol{p}_1) = h(\boldsymbol{p}_2)] = 1 - \frac{\theta(\boldsymbol{p}_1, \boldsymbol{p}_2)}{\pi}. \tag{2.9}$$

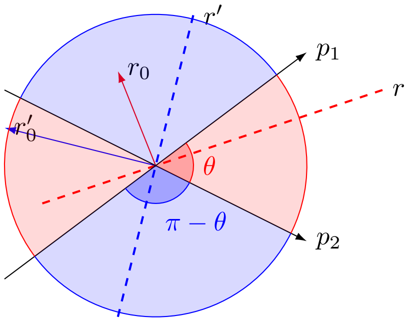

Figure 2.9: Visual Proof of claim in equation 2.9

For a visual proof of the claim in Equation 2.9 consider Figure 2.9, where two vectors $\boldsymbol{p}_1$ and $\boldsymbol{p}_2$, regardless of their dimensionality, define a plane and an angle $\theta$ in this plane. Pick a hyperplane $r$ that intersects the plane that is spanned by $\boldsymbol{p}_1$ and $\boldsymbol{p}_2$ in a line (depicted as a red dashed line). Actually, a normal vector $r_0$ is randomly selected and $r$ is the set of points whose dot product with $r_0$ is zero. Since $\boldsymbol{p}_1$ and $\boldsymbol{p}_2$ are on different sides of the hyperplane, their projections given by $\boldsymbol{p}_1^\top r_0$ and $\boldsymbol{p}_2^\top r_0$ will have different signs. Such a scenario, where two points have different signs, is interpreted as a notion of dissimilarity. Thus, the hyperplane acts as a clustering primitive that partitions the original input set into two disjunct sets.

The opposite scenario is illustrated by a random normal vector $r'_0$ that is normal to the hyperplane $r'$, which is represented by the blue dashed line. Both $\boldsymbol{p}_1^\top r'_0$ and $\boldsymbol{p}_2^\top r'_0$ will have the same sign. This in turn is interpreted as a notion of similarity, since both points are clustered into the same set. All angles between the intersection line of the random hyperplane and the plane spanned by $\boldsymbol{p}_1$ and $\boldsymbol{p}_2$ are equally likely. Thus, the probability that the hyperplane looks like the red line is $\theta/\pi$ and like the blue line $1-\theta/\pi$.

Therefore, GRP is a $(r, cr, (1-r/\pi), (1-cr/\pi))$-sensitive family for any $r$ and $cr$. As already explained in Section 2.2.2, such a family can be amplified as desired. The AND-construction is refers to the selection of a number of $K$ different random hyperplanes $r_k$. According to the construction in Equation 2.7, all projections $\boldsymbol{p}_n^\top r_k$ for a single point are concatenated into a $K$-bit vector. Likewise, the OR-construction refers to the initialization of a number of $L$ such AND-constructions. The algorithmic procedures for preprocessing and queries from Algorithm 1 and Algorithm 2 can be applied withoud change.

## 2.3 Gaussian Mixtures

This section focuses the concept of GMM for density estimation. For this purpose, the Gaussian normal distribution is presented first, by introducing basic definitions for the probability density functions and describing the closure properties of the distribution. For this purpose, at the beginning a short motivation for the application of the presented model will be given. Then, mixture models in general and GMM in particular are defined. After that, two main concepts will be explained. First, the GMM is interpreted in terms of a LVM. Second, the EM Algorithm is presented, which performs the computation of model parameters of latent variable models in an iterative scheme.

## 2.4 Principal Component Analysis

### 2.4.1 Dimensionality Reduction

This chapter focuses on dimensionality reduction of data in the context of Principal Component Analysis. First, the application of dimensionality reduction in general is motivated by various examples. Then, the core idea based on the separation of signal and noise in data is presented. After this, a concrete statement of the problem is introduced. In addition, key model assumptions and a solution approach is presented and followed by a mathematical derivation of the eigencomposition for solving Principal Component Analysis (PCA). Finally, a particular example is given.

#### Motivation

Several difficulties arise when analyzing high-dimensional data [DFO20, p.286]. For example, it is often not easy to interpret which of the many factors have the most significant influence on the data distribution. In addition, data visualizations are often limited to a few dimensions. And besides the impact on data analysis, there are also influences on data inference.

Some machine learning algorithms cannot effectively reason about the underlying structure of the data in high-dimensional space, which can result into a model overfitting. Furthermore, compression of data, in terms of dimensionality reduction, can lead to advantages in processing and persistence of data. Data storage can often come at a high cost and some algorithms do not scale well with increasing numbers of dimensions. For example, when using the Expectation Maximization Algorithm (EM Algorithm) (see Chapter **??**) increasing dimensionality of the data is related to an increase in the probability of the occurrence of (nearly) singular matrices, which can result in a numerical breakdown of the model [Bis06, p.434]. For these reasons, dimensionality reduction is often desired within a data preprocessing strategy.

### 2.4.2 Signal and Noise

In general, dimensionality reduction methods make use of the following idea. Measuring data is error prone and associated with both incompleteness and redundancy. This trend increases with the number of measurement points, i.e. dimensions. Thus, many dimensions in multivariate data can be explained by a combination of other dimensions. This underlying structure can be exploited by partitioning the full space into subspaces of signal and noise [**sco_2015**]. Figure **??** shows two randomly created datasets. The plot on the right displays a negative correlation and the direction that carries the largest portion of the signal can be located visually. In this two-dimensional example, the direction that is perpendicular to that is the direction that carries the least amount of signal and is referred to as noise. The goal is to discard a significant amount of noise in the data and work with a more compact representation, with losing as little signal as possible.

#### Problem Setting

All data points $\boldsymbol{x}_n$ can be represented as a linear combination of the orthonormal basis. Considering an example dataset with three dimensions, the orthonormal basis of $\mathbb{R}^3$ is the canonical basis $e_1 = [1,0,0]^T, e_2 = [0,1,0]^T, e_3 = [0,0,1]^T$.

The central question associated with PCA is whether there is another basis, which is a *linear* combination of the original basis, that best represents the data. From this perspective, PCA can be considered a change-of-basis problem. Recalling the example from Figure **??**, a better representation of the data is related to a lower amount of noise and redundancy in the data. Further, by assuming linearity, the problem is simplified by restricting the set of potential bases and enabling an efficient solution with matrix decomposition techniques [**shl_2014**].

It is not always the case that the correlation among variables is not of interest. But in the case of PCA, correlation represents redundancy, which is desired to be minimized.

**Assumptions and Solution Approach**

To derive a solution approach, some assumptions are made beforehand, which are proven in the following chapter. It is assumed that data containing more redundancy generally have lower variance and vice versa. Therefore, the dynamics of interest exist in the directions of highest variance. It is further assumed that the canonical basis in which the data was recorded is a representation that has inherent redundancies and noise. For this reason, a suitable basis is searched that represents a linear transformation of the canonical basis, such that the base aligns with the axes of maximum variance of the data. By projecting the data onto the axis of maximum variance, which form a lower-dimensional subspace, data redundancy is eliminated.

Finding the directions of maximum variance, which are referred to as principal components, is the central operation of PCA. One feasible option is to diagonalize the covariance matrix of the data. Recalling that each covariance matrix is a square symmetric matrix whose off-diagonal elements represent the covariances, i.e. reflect the redundancies, a diagonalization of the covariance matrix eliminates the magnitude of the covariance, resulting in a matrix that only contains the variance terms. Finally, each successive dimension in the diagonalized covariance matrix should be rank-ordered according to the values of the variance in order to quantify their importance.

It can be shown that the principal components are the eigenvectors of the covariance matrix of the data. A frequently used method for solving PCA is therefore the eigendecomposition, which is mathematically derived in the following in connection with the assumptions made so far.

### 2.4.3 Formal Description

Consider a dataset $\boldsymbol{X} = \{\boldsymbol{x}_1, \ldots, \boldsymbol{x}_n\} \in \mathbb{R}^D$ with mean $\mathbf{0} = [0_1, \ldots, 0_n]^T$ and covariance matrix

$$\boldsymbol{C} = \frac{1}{N} \sum_{n=1}^{N} \boldsymbol{x}_n \boldsymbol{x}_n^T.$$

In terms of dimensionality reduction, a compressed representation of the dataset $\boldsymbol{X}$ as

$$\boldsymbol{z_n} = \boldsymbol{B}^T \boldsymbol{x}_n \in \mathbb{R}^M$$

is searched for, which retains as much of information as possible (Hotelling 1933). This is done by finding a linear transformation

$$\boldsymbol{B} = [\boldsymbol{b}_1, \ldots, \boldsymbol{b}_M] \in \mathbb{R}^{D \times M}$$

that projects $\boldsymbol{X}$ onto the subspace that is spanned by the columns of $\boldsymbol{B}$. Thus, $\boldsymbol{B}$ is an orthonormal basis.

**Definition 8** (Orthonormal Basis)**.** [DFO20, p.65] Let $V$ be a $n$-dimensional vector space with a basis $\{b_1, \ldots, b_n\}$. The basis is called an Orthonormal Basis (ONB) if

$$\langle b_i, b_j \rangle = 0 \text{ for } i \neq j,$$
$$\langle b_i, b_j \rangle = 1.$$

In order to preserve the most variance of the data, the basis vectors of $\boldsymbol{B}$ must point into the direction of maximal variance in the data, which is found by computing the eigenvectors of the covariance matrix $\boldsymbol{C}$ of $\boldsymbol{X}$. The projection of the data onto a lower-dimensional subspace is equal to the eigenvalue that is associated with the basis vector that spans this subspace.

Therefore, maximizing the variance of the low-dimensional representation $Z$ requires to choose the basis vector that is associated with the largest eigenvalue of the data covariance matrix. This eigenvector is called the first principal component. All other directions in $\mathbb{R}^M$, which both maximize the variance and are orthogonal to all the other directions are the remaining $M - 1$ principal components.

As stated before, the projection matrix $\boldsymbol{B}$ is obtained by diagonalizing the covariance matrix $\boldsymbol{C}$, which can be done with via eigendecomposition. In the following, it is shown how the eigendecomposition is related to the diagonalization of a matrix and that an eigendecomposition of a covariance matrix is guaranteed to exist.

**Theorem 9** (Matrix Diagonalization)**.** [DFO20, p.98] A matrix $A \in \mathbb{R}^{n \times n}$ is diagonalizable if it is similar to a diagonal matrix, i.e. if there exists an invertible matrix $P \in \mathbb{R}^{n \times n}$ such that $D = P^{-1}AP$.

**Theorem 10** (Eigendecomposition)**.** [DFO20, p.99] A square matix $A \in \mathbb{R}^{n \times n}$ can be factorized into

$$A = PDP^{-1},$$

where $P \in \mathbb{R}^{n \times n}$ and $D$ is a diagonal matrix whose entries are the eigenvalues of $A$, if and only if the eigenvectors of $A$ form a basis of $\mathbb{R}^n$.

It follows, that only non defective matrices can be diagonalized. In other words, a square matrix that does not have a complete basis of eigenvectors is not diagonalizable. However, the following theorem confirms the existence of such a basis for symmetric matrices.

**Theorem 11** (Spectral Theorem)**.** [DFO20, p.94] If $A \in \mathbb{R}^{n \times n}$ is symmetric, there exists an orthonormal basis of the corresponding vector space $V$ consisting of eigenvectors of $A$, and each eigenvalue is real.

From the fact that every covariance matrix is symmetric, the following can be concluded.

**Theorem 12** (Diagonalization of a Symmetric Matrix)**.** A symmetric matrix $S \in \mathbb{R}^{n \times n}$ can always be diagonalized.

Therefore, it is assured that an eigendecomposition of a symmetric matrix $A$ exists (with real values), and that an ONB of eigenvectors can be found, so that $A = PDP^{-1}$, where $D$ is diagonal and the columns of $P$ contain the eigenvectors.

Rewriting the equation from Theorem 10 as follows reveals the eigenvalue equations:

$$A[p_1, \dots, p_n] = [p_1, \dots, p_n] \begin{bmatrix} \lambda_1 & 0 & 0 & \cdots & 0 \\ 0 & \lambda_2 & 0 & \cdots & 0 \\ 0 & 0 & \lambda_3 & \cdots & 0 \\ \vdots & \vdots & \vdots & \ddots & \vdots \\ 0 & 0 & 0 & \cdots & \lambda_n \end{bmatrix} \iff \begin{array}{ccc} Ap_1 & = & \lambda_1 p_1 \\ Ap_2 & = & \lambda_2 p_2 \\ Ap_3 & = & \lambda_3 p_3 \\ & \cdots & \\ Ap_n & = & \lambda_n p_n \end{array}$$

Next, it is shown how the eigenvalue equation shown above is related to the maximization of the variance of the data. For this purpose, the single vector $\boldsymbol{b}_1 \in \mathbb{R}^D$ is considered only, which is the first column of the matrix $\boldsymbol{B}$ and therefore the first of $M$ orthonormal basis vectors. By exploiting the i.i.d. assumption of the data, the first component of $\boldsymbol{z}_n \in \mathbb{R}^M$ of a single data point $\boldsymbol{x}_n \in \mathbb{R}^D$ is given by

$$z_{1n} = \boldsymbol{b}_1^T \boldsymbol{x}_n. \tag{2.10}$$

Thus, $z_{1n}$ is the coordinate of the orthogonal projection of $\boldsymbol{x}_n$ onto the one-dimensional subspace spanned by $\boldsymbol{b}_1$. Then, the variance of $z_{1n}$ of $\boldsymbol{z} \in \mathbb{R}^M$, that is maximized by $\boldsymbol{b}_1$, is defined as

$$V_1 := \mathrm{Var}[z_1] = \frac{1}{N} \sum_{n=1}^{N} z_{1n}^2. \tag{2.11}$$

The relation between the variance and the factorized matrix in Theorem 10 becomes evident by substituting equation (2.10) into equation (2.11) as

$$\begin{aligned} V_1 &= \frac{1}{N} \sum_{n=1}^{N} (\boldsymbol{b}_1^T \boldsymbol{x}_n)^2 \\ &= \frac{1}{N} \sum_{n=1}^{N} \boldsymbol{b}_1^T \boldsymbol{x}_n \boldsymbol{x}_n^T b_1 \\ &= \boldsymbol{b}_1^T (\frac{1}{N} \sum_{n=1}^{N} \boldsymbol{x}_n \boldsymbol{x}_n^T) \boldsymbol{b}_1 \\ &= \boldsymbol{b}_1^T \boldsymbol{C} \boldsymbol{b}_1. \end{aligned} \tag{2.12}$$

By maximizing the variance defined in (2.12) results in finding vector $\boldsymbol{b}_1$. But arbitrarily increasing the magnitude of $\boldsymbol{b}_1$ increases $V_1$, which is why restricting all solutions to unit vector size is necessary:

$$||\boldsymbol{b}_1||^2 = 1 \Leftrightarrow ||\boldsymbol{b}_1|| = 1.$$

Restricting the solution space results into a constrained optimization problem :

$$\begin{aligned} \max\ &\boldsymbol{b}_1^T \boldsymbol{C} \boldsymbol{b}_1 \\ \text{s.t.}\ &||\boldsymbol{b}_1||^2 = 1. \end{aligned}$$

By applying the method of Lagrange multipliers, the new objective function is obtained as

$$\mathcal{L}(\boldsymbol{b}_1, \lambda) = \boldsymbol{b}_1^T \boldsymbol{C} \boldsymbol{b}_1 + \lambda_1 (1 - \boldsymbol{b}_1^T \boldsymbol{b}_1).$$

The partial derivative of $\mathcal{L}$ with respect to $b_1$ gives

$$\begin{aligned} \frac{\partial \mathcal{L}}{\partial \boldsymbol{b}_1} &= 2\boldsymbol{b}_1^T \boldsymbol{C} - \lambda_1 \boldsymbol{b}_1^T \\ 0 &= 2\boldsymbol{b}_1^T \boldsymbol{C} - \lambda_1 \boldsymbol{b}_1^T \\ \boldsymbol{C}\boldsymbol{b}_1 &= \lambda_1 \boldsymbol{b}_1. \end{aligned}$$

By the definition shown above, $\boldsymbol{b}_1$ has to be an eigenvector of $\boldsymbol{C}$ with the lagrangian multiplier as corresponding eigenvalue. Then, computing the derivative with respect to $\lambda_1$ results in

$$\begin{aligned} \frac{\partial \mathcal{L}}{\partial \lambda_1} &= 1 - \boldsymbol{b}_1^T \boldsymbol{b}_1 \\ 0 &= 1 - \boldsymbol{b}_1^T \boldsymbol{b}_1 \\ \boldsymbol{b}_1^T \boldsymbol{b}_1 &= 1. \end{aligned}$$

Finally, the variance objective from equation (2.12) can be rewritten as

$$V_1 = \boldsymbol{b}_1^T \boldsymbol{C} \boldsymbol{b}_1 = \lambda_1 \boldsymbol{b}_1^T \boldsymbol{b}_1 = \lambda_1. \tag{2.13}$$

The variance of the projected data equals the eigenvalue that is related to the basis vector $\boldsymbol{b}_1$, which spans the subspace the data is projected onto. In other words, the eigenvector that is associated with the biggest eigenvalue $\lambda_1$ is the first principal component.

Since the vector $\boldsymbol{b}_1^T$ is considered a linear transformation, computing its inverse projects $z_{1n}$ back into the original data space $\mathbb{R}^D$, such that

$$\tilde{\boldsymbol{x}}_n = \boldsymbol{b}_1 z_{1n} = \boldsymbol{b}_1 \boldsymbol{b}_1^T \boldsymbol{x}_n.$$

So far, only the solution for the first principal component has been derived. Generalizing this schema onto a $M$-dimensional subspace with maximal variance involves some way of mathematical induction. The idea is to subtract the effect of the first $M - 1$ principal components $\boldsymbol{b}_1, \ldots, \boldsymbol{b}_{M-1}$ from the data and thereby trying to find the principal components that compress the remaining information. For a detailed investigation of this general case, reference is made to [DFO20, pp.291]

# Chapter 3

# State of the Art

## 3.1 Data Dissemination in Collaborative Intrusion Detection

## 3.2 Similarity Hashing in Malware Detection

## 3.3 Generative Algorithms and Intrusion Detection

# Chapter 4

# Generative Pattern Database

Three main challenges in the context of data dissemination in CIDS were identified. First, intrusion related data is usually of sensitive nature. Thus, the exchange mechanism must not compromise any policies and regulations related to data *privacy*. At the same time, the usability of the data has to be preserved. Second, the data that is subject of the exchange may exhibit large volumes. That constitutes a challenge, since the dissemination is desired to be executed with *minimal overhead* in a timely and scalable fashion. Lastly, the *interoperability* of the CIDS with existing local IDS is an important aspect that influences the practical adoption into security architectures. In summary, existing approaches for data dissemination mainly provide mechanisms for exchanging alert data or single attributes, e.g. IP addresses, as they focus on the correlation of intrusion detection incidents that originate from different sensors. The exchange of actual training data is neglected, possibly due to high data volumes. Thus, these systems lack of mechanisms for the extraction and global persistence of novel attack patterns, e.g. from zero day exploits, that can be used for the training of an intrusion detection sensor.

The approach that is presented in this chapter exchanges attack patterns by sharing generative machine learning models that have been trained on partitions of similar data points. Such a model-based dissemination enables the receiving side to sample a synthetic dataset that enhances existing local datasets. This provides two main advantages. First, no original data leaves a local network and therefore does not violate any privacy restrictions. Second, the data is compressed considerably by representing it in form of a generative model. In order to make that mechanism scalable, the monitored data is clustered using random projections. This way, similar data points are partitioned into globally common clusters, which is exploited as a data parallelism mechanism. Given that, bursty workloads can be served effectively in a cloud deployment. Furthermore, this mechanism enables a similarity-based correlation of distributed intrusion events. The integration of both a similarity based correlation of intrusion incidents and a mechanism for sharing attack knowledge makes it possible to extract novel patterns of distributed attacks and provide them globally within the CIDS, resulting in an improved attack detection.

Section 4.1 introduces the idea and key concepts of the approach. After that, Section 4.2 specifies the proposed architecture in detail. A comprehensive description of algorithms and processing steps are described in Section 4.3.

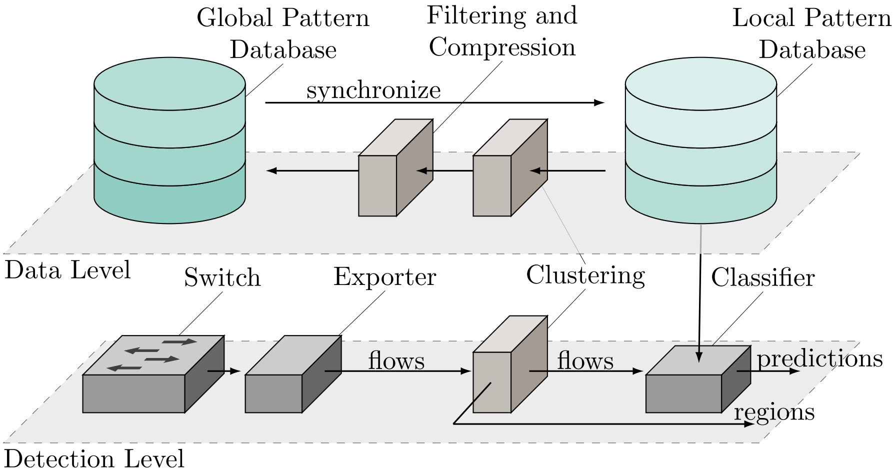

Figure 4.1: Example integration of the generative pattern database into a generic NIDS deployment, seperated by data and detection level

## 4.1 High Level Overview

Several members exist in the CIDS, each of which manages an isolated IDS. Every IDS operates according to a specific set of rules, that is essentially based on the content of a local database. The goal of the generative pattern database is to close the knowledge gaps of local databases and thus increase the detection rate of associated IDSs. By providing a *global view* on all local databases, individual IDSs can benefit from the collective knowledge of the CIDS.

Section 4.1.1 starts with a reference example to illustrate the idea that is described above and discusses the integration of the CIDS into existing infrastructures. Subsequently, Section 4.1.2 and Section 4.1.3 show the key concepts that enable data distribution and correlation under the given requirements. Finally, Section 4.1.4 combines the individual elements to present the strategy for the creation and utilization of the global view.

### 4.1.1 Example Integration

An exemplary integration of the CIDS into a generic NIDS is shown in Figure 4.1. The exemplary NIDS deployment consists of three components, that can be found on the detection layer. A flow exporter computes statistical flow features based on the network packets of a switch. A discriminative model serves as a classifier that operates on the specific feature set that the exporter extracts. After completing the training of a classifier instance on a given dataset, it is deployed within the detection pipeline. There, the classifier receives a stream of network flows and predicts them.

The CIDS mainly integrates at the data level, where the training data for the classifier is provided by the *local pattern database*. At this point, the local pattern database only contains the *local view* of the intrusion detection data from that particular member. In order to provide a global view, a synchronization process between its local pattern database and the *global pattern database* has to be initiated. Before the data is transferred to the global pattern database, it is subject to a set of clustering, filtering and compression operations. This way, data privacy is maintained and overhead is minimized by reducing the data volume.

On the receiving side, the global pattern database combines data from all members into a global view. Upon each update of the global pattern database, the new state of the global view is synchronized to each local pattern database and subsequently enhances the classifier on the detection level by extending the local intrusion detection dataset. Furthermore, an identical clustering operation as on the data level is applied on the detection level. Each incoming flow is assigned to a certain cluster, which is referred to as *region*. While the predictions from the classifier are suitable for detecting attacks that are known to the CIDS, regions are leveraged for the detection of novel data patterns and similarity-based correlations that uncover large-scale coordinated attacks, which are executed on the resources of multiple CIDS members simultanously.

### 4.1.2 Clustering

The clustering operation has to meet certain requirements in this approach.First, the results of the clustering operation should be consistent while it is executed among all members of the CIDS in a distributed fashion. Additionally, the algorithm should be scalable, since it is to be applied on whole databases on the data level and on streams of live data on the detection level. Given these requirements, gaussian random projection (GRP) (see Section 2.2.3) is selected. By using GRP, real data points are clustered according to their angular distance. Furthermore, the projection result is a binary string, which can be used for storing similar data points into a common bucket of a hash table by using the binary string as an index. In the context of the generative pattern database, the combination of GRPs and hash tables is exploited as the main controlling primitive for data persistence and retrieval. Instead of using randomly selected projection planes, a shared seed results in the application of a common projection function among all members of the collaboration. In other words, similar data points from different datasets are indexed to a common global bucket, i.e. region. Each region is subject to the transformations individually, which is utilized as a data parallelism mechanism. Thus, this approach is natively suited for cloud deployments where bursty workloads can be served effectively by balancing the load on an arbitrary number of instances. Lastly, this mechanism enables a similarity-based correlation of distributed intrusion events. As incoming data is monitored on the detection level, the clustering is applied, which results in a pattern that can be used for novelty checks or global occurrences within the CIDS.

### 4.1.3 Filtering and Compression

Two types of data are extracted within individual regions. First, metadata of local datasets is collected by counting label occurrences, which serve as indicator for determining if the respective region needs to be subject to the second extraction type. Second, models that are trained with generative algorithms on local attack data are the exchange medium for disseminating information within the CIDS. This provides two main advantages. For one, no original data leaves a local network and therefore does not violate any privacy restrictions. For another, the data is compressed considerably by representing it in form of a generative model.

### 4.1.4 Global View

As shown in Figure 4.2, each view is partitioned by a common projection function into an identical set of regions. Each local view contains original datapoints from the local dataset of the respective CIDS member. In this example, there exist three different classes globally, which occur differently in each local dataset. Examining a specific region, the combination of unique classes within all local views determines its complexity on a global level. For instance, the yellow region (global view) is simple, because within all local views, there occurs only a single class. A complex region in the global view, on the other hand, is formed by the occurrence of multiple classes within the same region in all local views. If a region in the global view contains more than one class, it potentially exhibits a non-linear decision boundary, hence it is called complex. This complexity information is distributed to all members of the CIDS by tagging the corresponding local regions with the complexity state of the region from the global view. After that, all local regions that are tagged as complex are modeled by a generative algorithm by using the corresponding local data points as training data. Subsequently, the resulting models are transferred to the global view. A synchronization process disseminates the region complexity estimations and the generative models to all local views. Within each local view, data points are sampled from generative models which are subsequently assembled into a synthetic dataset. Finally, the synthetic datasets are blended into the respective local datasets for enhancing the subsequent training of discriminative models.

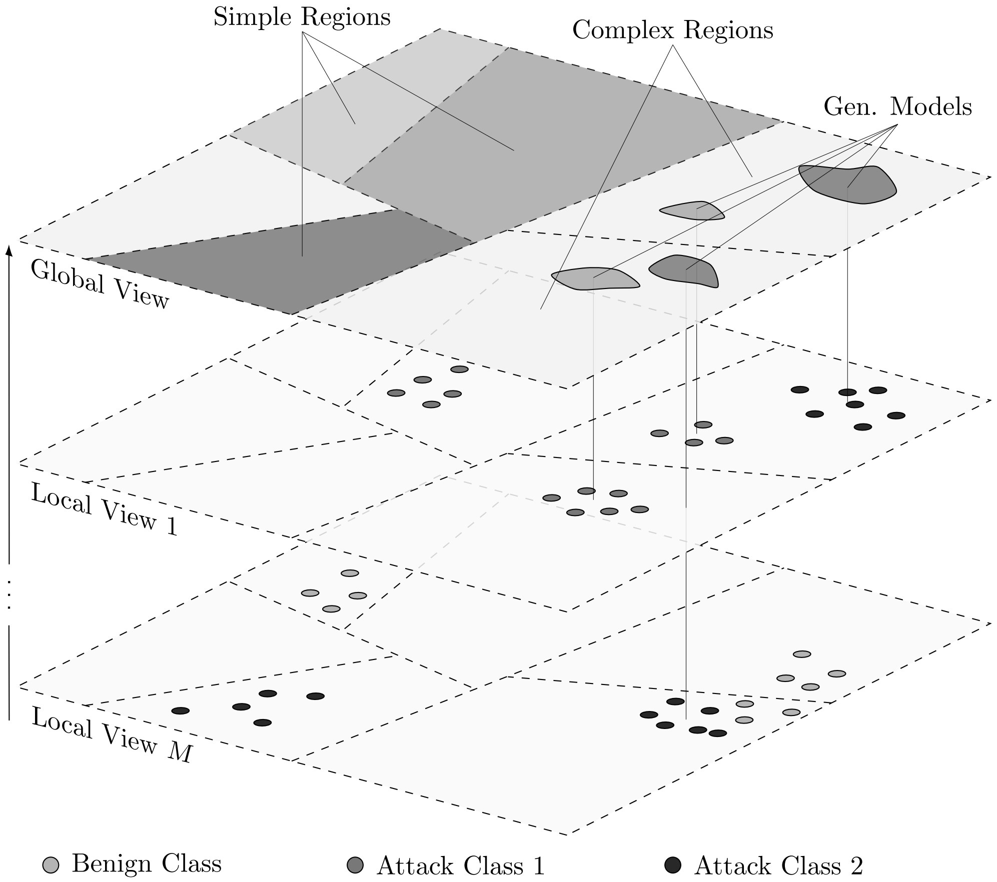

Figure 4.2: Building the global view by combining $M$ local views

## 4.2 Architecture Specification

Logically, the proposed CIDS exhibits a hierarchical architecture (see Figure 4.3). For one, the global infrastructure $G$ represents the collection of $M \in \mathbb{N}$ CIDS participants and their knowledge on an abstract level. For another, it provides specific services, that are globally available to each local infrastructure $L_m, m \in \{1, \dots, M\}$ that includes all CIDS components and services within the IT infrastructure boundaries of a corresponding CIDS member. Each local infrastructure $L_m$ agrees to a specified feature extraction process that provides the monitoring data $\mathcal{X} \subset \mathbb{R}^D$ with a total number of features $D = |\boldsymbol{x}| \in \mathbb{N}$ for the attack detection. As the deployed NIDS is considered to be a supervised classification task, the ultimate goal is to find an approximation of an unknown target function $c : \mathcal{X} \rightarrow \mathcal{Y}$ that maps examples $\boldsymbol{x} \in \mathcal{X}$ to classes $y \in \mathcal{Y}$. In order to find an approximation $\hat{c} \sim c$, an individual training dataset $\mathcal{D}_m = \{(\boldsymbol{x}_n, y_n) : 1 \leq n \leq N_m\}$ of size $N_m = |\mathcal{D}_m| \in \mathbb{N}$ is provided in every $L_m$. True target values $c(\boldsymbol{x}) = y$ are given by the domain expert that assembled $D_m$. In addition, in the CIDS network, a common $\mathcal{Y}$ is agreed upon, so that there is a global consensus on class memberships.

CIDS communication across local boundaries occurs exclusively in a vertical direction. Thus, the exchange of information between individual $L_m$ takes place indirectly via the global pattern database ($PDB_G$) and the global event channel ($C_G$). Each $L_m$ includes a local pattern database ($PDB_{L_m}$), a local event channel ($C_{L_m}$) and an event-based data processing pipeline that consists of four services, namely *Local Indexing*, *Complexity Estimation*, *Generative Fitting* and *Classifier Fitting*.

Each instance of a pattern database ($PDB$) is realized as a key-value store and depending on the scope different tasks are considered. Each $PDB_{L_m}$ is responsible for storing $D_m$ and corresponding metadata. The $PDB_G$ stores global metadata and the generative models that resemble the original data from each $D_m$. The notation for operations on a $PDB$ corresponds to the notation for hash table operations defined in Section 2.2.2. Note, that if a locality-sensitive hash function is used to construct a key, in practice a hash table will internally apply a non-cryptographic hash function on the key to ensure an even distribution of the keys across the slots.

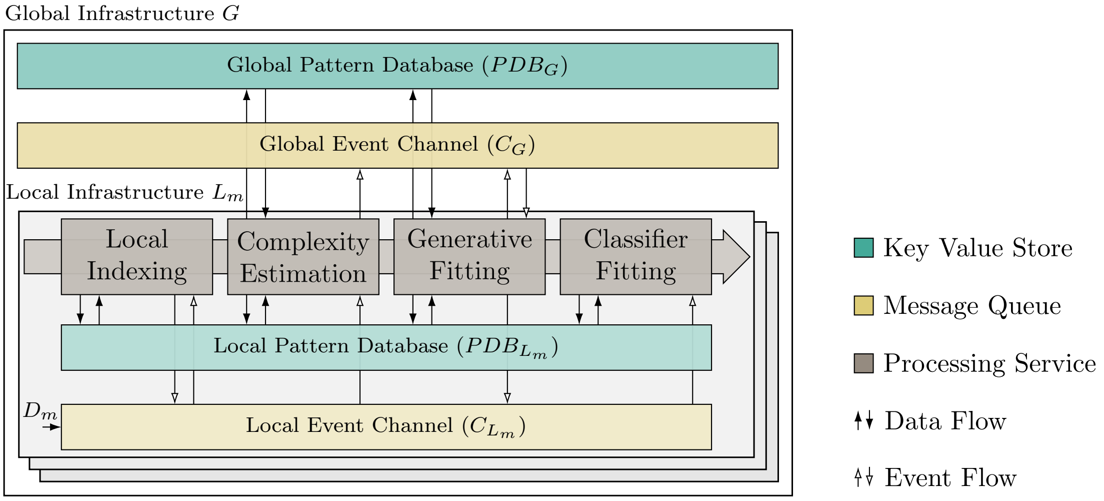
Global Infrastructure $G$
Global Pattern Database ($PDB_G$)
Global Event Channel ($C_G$)
Local Infrastructure $L_m$
Local Indexing
Complexity Estimation
Generative Fitting
Classifier Fitting
Local Pattern Database ($PDB_{L_m}$)
$D_m$
Local Event Channel ($C_{L_m}$)
Key Value Store
Message Queue
Processing Service
Data Flow
Event Flow

Figure 4.3: CIDS architecture illustrating the data and event flow between components within and across local infrastructure boundaries

Nonetheless, the clustering of neighbouring points into common slots is still ensured in this scenario. Each event channel $C$ provides a topic-based publish-subscribe messaging mechanism that is mainly used to instantiate and distribute workloads among the service instances in the processing pipeline. Via the messaging system, service instances receive and emit events, on which upon the respective operations are triggered. Changes in a $PDB$ result in responses that in turn are leveraged as the respective events. In this fashion, updates are propagated throughout the processing pipeline, ensuring a timely consistency among the pattern databases.

## 4.3 Service Specification

In Section 4.1, the roles of the clustering, filtering and compression operations within the architecture and the idea of the global view have been roughly explained. These concepts are implemented within the processing pipeline that has been referred to in Section 4.2 as four consecutive and event-based services, which are described in detail by focusing on a single service in each subsection.

### 4.3.1 Local Indexing

The local indexing service is responsible for the preprocessing and local storage of $D_m$. As already described in Section 4.1.2, the data is organized in regions. This means that individual data points are first assigned to a region using a GRP. By doing that, a hash of the data point is computed. Based on the generated hash value, a key is constructed that is used to persist that data point in the respective $PDB_{L_m}$. According to the properties of a locality-sensitive hash function, similar data points are assigned to a common region and thus form a closed processing unit for subsequent operation steps. If a region is initialized or an update is made to an existing region, e.g., due to the occurrence of new data, events are emitted to inform the subsequent service.

First, an intrusion detection dataset $D_m$ is sent to one or more service processors via the $C_{L_m}$. Second, the incoming stream of pairs of data points and labels $(\boldsymbol{x}_n, y_n) \in D_m$ is ingested and buffered until a batch $X = (\boldsymbol{x}_1, y_1), \ldots, (\boldsymbol{x}_B, y_B)$ of size $B \in \mathbb{N}$ has been accumulated. Then, $X$ is preprocessed and inserted into the $PDB_{L_m}$ as described in Algorithm 3. In words, a flow-feature vector $\boldsymbol{x}$ is scaled to the range $[-1, 1]$ by applying a feature-wise min-max normalization given by

$$\boldsymbol{x}' = (b - a)\, \frac{\boldsymbol{x} - \min \boldsymbol{x}}{\max \boldsymbol{x} - \min \boldsymbol{x}} + a \tag{4.1}$$

where $a = -1$ and $b = 1$. After that, the scaled data point $\boldsymbol{x}'$ is subject to both a locality-sensitive hashing function $h$ and a non-cryptographic hashing function $g$. In this particular architecture, $h$ is a GRP with a global seed for the initialization of the projection plane $\boldsymbol{M}$ (see Section 2.2.3), such that regions $r = h(\boldsymbol{x}')$ across local infrastructures are comparable and consistent.[1] Since the data is organized in regions, a nested scheme is applied for the insertion of pairs of datapoints and labels as depicted in Figure 4.4.

[1] Here, the words hash value and region are used synonymously

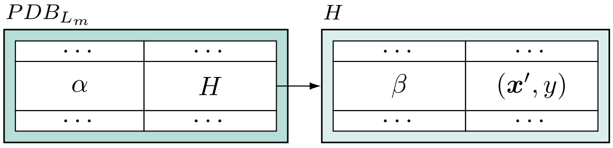

Figure 4.4: Nested indexing in a local pattern database.

In fact, the pairs within a region are further partitioned into disjoint subsets according to the true class label $y$. This means that for each subset of the data of a particular label within a region, a separate hashtable is initialized and inserted into the $PDB_{L_m}$ as a second level. Thus, for the persistence of a pair $(\boldsymbol{x}', y)$, two keys $\alpha, \beta$ are constructed (see Lines 6-7 in Algorithm 3). The key $\alpha$ is a concatenation of the prefix constant $p_x$, the bit-string $r$ and the label $y$. This way, the data is partitioned primarily by its region and secondarily by its label as described above. The key $\beta$ is the result of the non-cryptographic hashing function $g(\boldsymbol{x}')$, which serves as a mechanism for deduplicating identical $\boldsymbol{x}'$. Additionally, a third key $\gamma$ is constructed by concatenating the prefix constant $p_y$ and the bit-string $r$. As it is important to retrieve all existing labels within a region efficiently in a processing step of the subsequent service, $\gamma$ is used for storing the set of labels within a region as auxiliary metadata. Next, if not already present, a hash table is initialized and inserted into $PDB_{L_m}$ using $\alpha$. Likewise, if $PDB_{L_m}$ at slot $\gamma$ is empty, a new set[2] is initialited and inserted. After that, it is checked if the slot $\beta$ of the hash table placed at $\alpha$ in $PDB_{L_m}$, is empty. In the positive case, the pair $(\boldsymbol{x}', y)$ is inserted into that slot and the region $r$ is inserted into the set $\mathcal{R}$. Otherwise, no data is inserted into the local pattern database and no region is added to $\mathcal{R}$. After processing a batch, the set of updated regions $\mathcal{R}$ is emitted as events into $C_{L_m}$.

```
Input: Batch $X$
Output: Regions $\mathcal{R}$
 1: $\mathcal{R} \leftarrow$ new Set
 2: $\min \boldsymbol{x}, \max \boldsymbol{x} \leftarrow$ extract feature ranges from $X$
 3: for each $(\boldsymbol{x}, y)$ in a batch do
 4:     $\boldsymbol{x}' \leftarrow \text{normalize}(\boldsymbol{x})$                ▶ see Equation 4.1
 5:     $r \leftarrow h(\boldsymbol{x}')$
 6:     $\alpha \leftarrow \text{concatenate}(p_x, r, y)$
 7:     $\beta \leftarrow g(\boldsymbol{x}')$
 8:     $\gamma \leftarrow \text{concatenate}(p_y, r)$
 9:     if $PDB_{L_m}[\alpha]$ is None then
10:         $PDB_{L_m}[\alpha] \leftarrow$ new hash table $H$
11:     if $PDB_{L_m}[\gamma]$ is None then
12:         $PDB_{L_m}[\gamma] \leftarrow$ new set $\mathcal{S}_r$
13:     if $PDB_{L_m}[\alpha][\beta]$ is None then
14:         $PDB_{L_m}[\alpha][\beta] \leftarrow (\boldsymbol{x}', y)$
15:         insert $y$ into the set at $PDB_{L_m}[\gamma]$
16:         insert $r$ into $\mathcal{R}$
17: return $\mathcal{R}$
```

Algorithm 3: Preprocessing and inserting $B \subset D_m$ into $PDB_{L_m}$

[2] A set is a data structure describing an unordered collection with no duplicate elements.

### 4.3.2 Complexity Estimation

As described in Section 4.1.4, a region is said to be complex if it contains more than one unique label. Otherwise, a region is simple. Since the data within a region already represents a cluster created by a locality-sensitive hashing function $h$, the existence of multiple classes within a single region indicates a non-linear decision boundary. On that basis we differentiate how a region is processed in the subsequent services of the pipeline. Furthermore, the complexity state of a region may vary, depending on the scope it is observed. Note that since the projection matrix $\boldsymbol{M}$ that is used to construct $h$ is initialized with the same values in every $L_m$, all hashes that were computed by $h$ are globally comparable. This means that similar data points from different datasets, e.g., $\boldsymbol{x}_i \in D_1$ and $\boldsymbol{x}_j \in D_2$, $\boldsymbol{x}_i \sim \boldsymbol{x}_j$ may be hashed to the same region $h(\boldsymbol{x}_i) = h(\boldsymbol{x}_j)$. However, it is also possible that that the corresponding labels $y_i \in D_1$ and $y_j \in D_2$ are not equal. Thus, a certain region may contain only a single unique label in both local scopes but multiple unique labels in the global scope and therefore lead to a different global view on that region's complexity state. Given that, the complexity estimation service acts as a bridge between the local and global components and answers the question, which regions are considered to be complex in a global scope.

First, a set of incoming regions $\mathcal{R}_{\text{in}}$ is received on the $C_{L_m}$. Then, for each region $r \in \mathcal{R}_{\text{in}}$ the following operations are executed (see Algorithm 4). The set of unique labels $\mathcal{S}_r$ for a particular region within a local scope has been stored in Algorithm 3 as auxiliary metadata, which is now retrieved from the $PDB_{L_m}$ by constructing the correspoding key $\gamma$. In the next step, $\mathcal{S}_r$ has to be stored in the $PDB_G$. Therefore, another key $\delta$ is constructed by concatenating the prefix constant $p_y$, the region $r$ and the current local infrastructure identifier $m$, which prevents the collision of information from different infrastructures. After $\mathcal{S}_r$ is stored on a global level at $PDB_G[\delta]$, the label set information for that region from all members in the CIDS is aggregated. That aggregated view is essentially the global complexity state for that region. By iterating over all member identifiers in the CIDS, multiple keys $\delta$ are constructed. Each key retrieves the specific label set $\mathcal{S}_r$ of a member and inserts its content into the temporary set $\mathcal{S}_t$, collecting the local label sets.

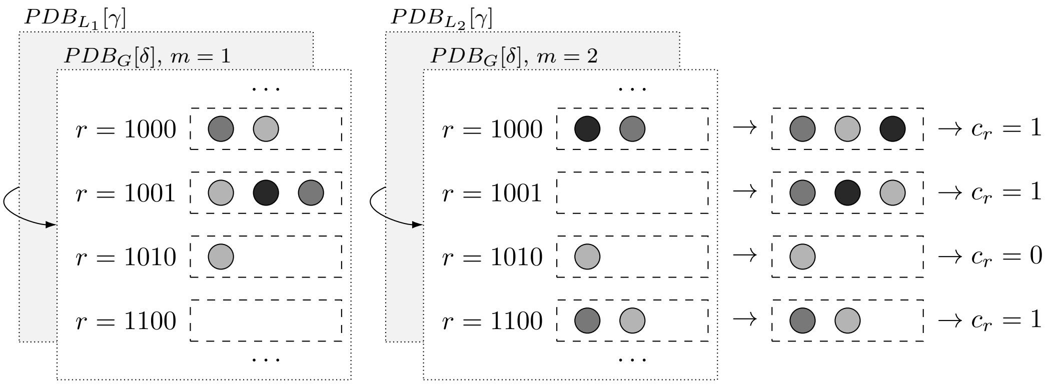

Figure 4.5: Illustration of the complexity estimation algorithm with two local infrastructures. Each local label set at $PDB_{L_m}[\kappa]$ is synchronized into the global pattern database at $PDB_G[\delta]$, where $\delta$ is constructed with $m$. Per region, the union operation is applied on the global label sets, whereupon the complexity is derived from.

After collecting all label sets in $\mathcal{S}_t$, the complexity state is obtained by simply evaluating the cardinality $|\mathcal{S}_t|$. If there is more than one class in a region on a global scope, that is $|S| > 1$, then assign a true value to the global complexity variable $c_r$. Otherwise, assign a false value. In order to store $c_r$, the key $\kappa$ is created by concatenating the prefix constant $p_c$ and the region $r$. Note, that $PDB_G[\kappa]$ is only updated, if storing $c_r$ changes the state that is already persisted. This is because, if an update is executed, this information has to be propagated to the next service. Thus, in that case, the region $r$ is inserted into $\mathcal{R}_{\text{out}}$, which is subsequently sent into the global event channel $C_G$ in order to inform services in all local infrastructures about the update.

```
Input: Regions $\mathcal{R}_{\text{in}}$
Output: Regions $\mathcal{R}_{\text{out}}$
$\mathcal{R}_{\text{out}} \leftarrow$ new Set
$m \leftarrow$ getID()                         ▶ current local infrastructure identifier
for each $r$ in $\mathcal{R}$ do
    $\gamma \leftarrow$ concatenate$(p_y, r)$
    $\mathcal{S}_r \leftarrow PDB_{L_m}[\gamma]$
    $\delta \leftarrow$ concatenate$(p_y, r, m)$
    $PDB_G[\delta] \leftarrow \mathcal{S}_r$
    $\mathcal{S}_t \leftarrow \emptyset$
    for each $m$ in $\{1, \dots, M\}$ do
        $\delta \leftarrow$ concatenate$(p_y, r, m)$
        $\mathcal{S}_t \leftarrow \mathcal{S}_t \cup PDB_G[\delta]$
    if $|\mathcal{S}_t| > 1$ then
        $c_r \leftarrow 1$
    else
        $c_r \leftarrow 0$
    $\kappa \leftarrow$ concatenate$(p_c, r)$
    if $PDB_G[\kappa] \neq c_r$ then
        $PDB_G[\kappa] \leftarrow c_r$
        add $r$ to $\mathcal{R}_{\text{out}}$
return $R_{\text{out}}$
```

Algorithm 4: Creating a global complexity state by combining local complexity states

### 4.3.3 Generative Fitting

The generative fitting service is the most demanding procedure in the context of processing resources. The service represents the filtering and compression operations presented in Section 4.1. There are two scenarios based on the region's complexity. If the region is not complex, no further actions are taken except it formally was complex. Then, existing models have to be deleted, since they are not longer used. And if the region is complex, generative models are provided, which represent the medium for exchanging information on attacks. More specifically, multiple Gaussian Mixture Model (GMM) are fitted on each label-subset of a region's data, which was stored in the indexing step in Section 4.3.1. According to a model selection process that evaluates the efficacy of each GMM, the best model is stored in the global pattern database, accessible to every member in the CIDS to sample synthetic data from.

This way, every member has access to the global knowledge from all local infrastructures in order to enhance the local dataset that is used for fitting a classifier. Thus, this service is the key for providing *privacy* and *minimal overhead* while exchanging information. Considering the length and complexity of the complete algorithm, the main procedure is outlined first in Algorithm 5 and then the details on important sub-routines are elaboreted subsequently.

Regions that have been updated in the preceding service are received as events $r \in \mathcal{R}_{\text{in}}$. Since the data is further organized per label within a region, the label set for a region $\mathcal{S}_r$ is retrieved. Additionally, the complexity state of the region $c_r$ is checked. Then, if the region is not complex, no model fitting is executed. Instead, potentially existing models are deleted from storage. This is the case, if the complexity status of the region has been changed from complex to simple. But if the region is currently complex, the generative model fitting procedure is triggered where new models are created and already existing models are updated. For that, from every hash table within a region, the original flow samples are extracted and collected in $\mathcal{X}_\alpha$, which is then stored in $T$ with the corresponding label as the key. The goal is to fit a model on each $\mathcal{X}_\alpha$ within a region, such that the collection of models for a region can be used in combination for sampling the synthetic data. Note that this is a specific process for the employed generativ algorithm. Since GMMs cannot be conditioned on multiple labels.

```
**Input:** Regions $\mathcal{R}_{\text{in}}$
**Output:** Regions $\mathcal{R}_{\text{out}}$
$\mathcal{R}_{\text{out}} \leftarrow \emptyset$
$m \leftarrow$ getID()
for each $r$ in $\mathcal{R}_{\text{in}}$ do
    $\kappa \leftarrow$ concatenate($p_c, r$)
    $\delta \leftarrow$ concatenate($p_y, r, m$)
    $c_r \leftarrow PDB_G[\kappa]$
    $\mathcal{S}_r \leftarrow PDB_G[\delta]$
    if $c_r = 0$ then
        for each $y$ in $\mathcal{S}_r$ do
            $\omega \leftarrow$ concatenate($p_d, r, y, m$)
            delete model in $PDB_G[\omega]$
    else
        $T \leftarrow$ new hash table
        for each $y$ in $\mathcal{S}_r$ do
            $\alpha \leftarrow$ concatenate($p_x, r, y$)
            $\mathcal{X}_\alpha \leftarrow$ extract values (flows) from $PDB_{L_m}[\alpha]$
            $T[y] \leftarrow \mathcal{X}_\alpha$
        $T \leftarrow$ upsampling($T$)
        for each $(y, F_y)$ in $T_F$ do
            GMM $\leftarrow$ modelSelection($y, F_y$)
            $\omega \leftarrow$ concatenate($p_d, r, y, m$)
            $PDB_G[\omega] \leftarrow$ GMM
        add $r$ to $\mathcal{R}_{\text{out}}$
return $\mathcal{R}_{\text{out}}$
```

Algorithm 5: Generative Fitting (Main Procedure)

Note that this is a specific process for the employed generative algorithm. Since GMMs cannot be conditioned on multiple labels, multiple single label models have to be fitted. Subsequently, upsampling operations prepare the collected region data in $T$ for the model fitting (see Algorithm 6). After that, the model selection process is started sequentially for each available label in the region (see Algorithm 7). Finally, the best fitted model is stored in the $PDB_G$.

So far, the main procedure has been outlined. Next, the details on the upsampling are elaborated (see Algorithm 6). As each $\mathcal{X}_\alpha$ is used for the fitting of a GMM and since some of these flow data subsets of a region potentially exhibit a low number of samples, an upsampling process may need to applied. The upsampling process ensures that the fitting algorithm for the GMM is able to work. For that, the number of samples has to be at least equal to the number of components of the GMM which in turn is at most equal to the number of dimensions of the training dataset $\mathcal{X}_\alpha$. And since different parameters for the number of components are tried during the model selection, the upper limit for the parameter is used as a comparison value. In this case the upper limit for the number of components is the number of dimensions of the training data. If this is not the case, the upsampling fills the lacking samples artificially.

For the initialization of the responsibilities of the mixture components within the fitting procedure of the GMM the k-means algorithm is used to find distinct clusters within $\mathcal{X}_\alpha$. The resulting cluster assignments for each $\boldsymbol{x} \in \mathcal{X}_\alpha$ are then used as initial values for the responsibilities. A supersampling process results in duplicate points that could lead to a smaller number if distinct clusters found by the k-means algorithm than the number of components specified in the model. Therefore, the upsampling is realized by generating near neighbours per sample.

First, the number of neighbours to generate per sample $N_\Delta$ is determined by dividing the difference of the dimensionality of the flow data $\dim(\mathcal{X}_\alpha)$ and the number of data points $|\mathcal{X}_\alpha|$ by $|\mathcal{X}_\alpha|$ using an integer division. This ensures that each original data point $\boldsymbol{x}$ contributes an equal share to the total amount of newly sampled points $\hat{\boldsymbol{x}}$. In case, the result of the integer division is zero, one is added to the result. Then for each data point $\boldsymbol{x} = [x_1, \ldots, x_D]^\top$, nearest neighbours are generated by sampling from a uniform distribution $\mathcal{U}(a, b)$.

```
Input: Hash table $T$ with labels $y$ as keys and sets of flows $\mathcal{X}$ as values
Output: Hash table $T$ with upsampled sets of flows
for each $(y, \mathcal{X}_\alpha)$ in $T$ do
    if $y \neq 0$ and $|\mathcal{X}_\alpha| < \dim(\mathcal{X}_\alpha)$ then
        $\hat{\mathcal{X}} \leftarrow \emptyset$
        $N_\Delta \leftarrow \lfloor \dim(\mathcal{X}_\alpha) - |\mathcal{X}_\alpha| \,/\, |\mathcal{X}_\alpha| \rfloor + 1$
        for each $\boldsymbol{x}$ in $\mathcal{X}_\alpha$ do
            for each $n$ in $\{1 \leq n \leq N_\Delta\}$ do
                $\hat{\boldsymbol{x}} \leftarrow [s(x_1), \ldots, s(x_D)]^\top$ with $s(x_d) \sim \mathcal{U}(a, b)$
                add $\hat{\boldsymbol{x}}$ to $\hat{\mathcal{X}}$
        $\mathcal{X}_\alpha \leftarrow \mathcal{X}_\alpha \cup \hat{\mathcal{X}}$
        $T[y] \leftarrow T[y] \cup \mathcal{X}_\alpha$
return $T$
```

Algorithm 6: Binary Splitting and Upsampling of Region Data

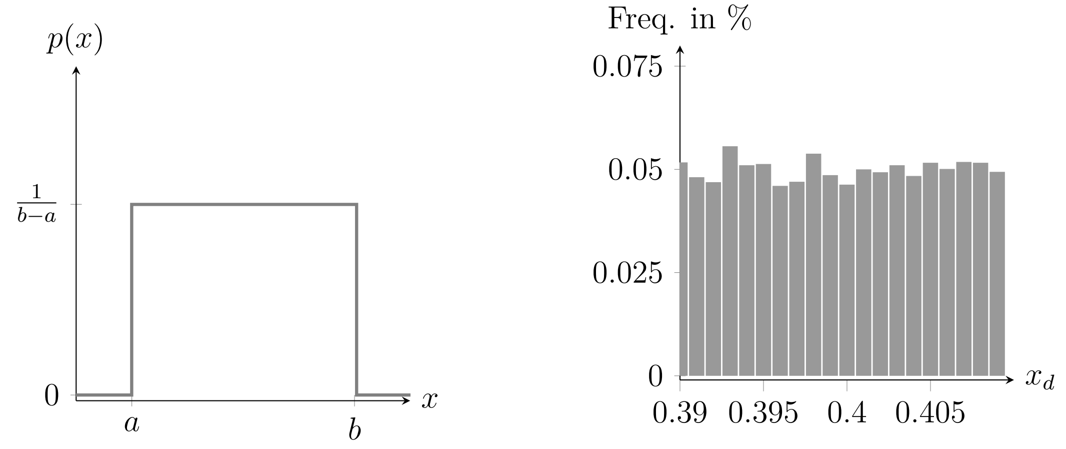

(a) The pdf of a uniform distribution is $p(x) = \frac{1}{b-a}$ within the interval $[a, b)$, and zero elsewhere.

(b) Histogram of 1 000 samples drawn uniformly over the interval $[x_d - \epsilon, x_d + \epsilon)$ where $x_d = 0.4$ and $\epsilon = 1 \cdot 10^{-2}$.

Figure 4.6: Nearest neighbours are generated by sampling each feature value from a the uniform distribution.

That way, the nearest neighbour of $\boldsymbol{x}$ is the concatenation of the sampled feature values as $\hat{\boldsymbol{x}} = [s(x_1), \ldots, s(x_D)]^\top$, where $s(x_d) \sim \mathcal{U}(a, b)$ is defined as the value sampled from the uniform distribution within the interval $[x_d - \epsilon, x_d + \epsilon)$. The value $\epsilon$ controls the size of the interval of the uniform distribution. The larger the value for $\epsilon$, the further the newly generated values deviate from the orginal feature values. In Figure 4.6b the value for a single feature $x_d$ is drawn uniformly at random. The original value of the feature was $x_d = 4$, which was extended by $\epsilon = 1 \cdot 10^{-2}$. By choosing a relatively small value for $\epsilon$, it is ensured that the generated nearest neighbours do not alter the original data distribution significantly, while enabling a more ideal fitting of the GMM for that set of data points. Finally, the generated neighbours and the original data points are combined. After processing each pair $(y, \mathcal{X}_\alpha)$, the hash table $T$ is returned to the main procedure (Algorithm 5) for the subseqeuent model selection.

In the next phase of the algorithm, one GMM is selected per unique label within a region. During the selection process multiple models are fitted with different model parameters using a flow data subset $\mathcal{X}_\alpha$. Since the resource demands of the EM Algorithm for fitting a GMM are relatively high, the dimensionality of the training data is reduced by applying a dimensionality reduction via PCA. Later in the pipeline, when sampling data from the GMMs, the inverse operation of the corresponding PCA is applied on the synthetic data in order to restore the original feature space. Therefore, the parameters of the PCA have to be stored in the $PDB_G$ along with the parameters of the GMM.

Note, that during the application of PCA in the first place, information within the data is lost by only keeping the components that describe most of the variance of the data. Of course, the result of the inverse transformation would then only be an approximation of the original data. However, the input for the inverse transformation is going to be the synthetic data. Thus, we accept the loss and focus on the fact that the synthetic data is transformed back into the original feature space. This way, the synthetic data resembles more the original data as it was captured and hence increases its compatibility.

The model selection is specified in Algorithm 7. First PCA is applied on $\mathcal{X}_\alpha$ resulting in a set of flows $\mathcal{X}'_\alpha$ with a reduced feature set. The number of components of the PCA has to be set heuristically or a threshold has to be set, which defines the minimum amount of variance that needs to be explained by a specific number of components. After the compression, the parameter search for the GMM is started. In general, there is no exact method to determine the optimal parameters for a GMM, such that different parameter settings have to be evaluated. For that, the search space is defined by two dimensions, namely the number of components and the type of covariance matrix that is used for each component. The set of numbers that is used for specifying the number of components is defined as $\mathcal{C} = \{4c \,|\, c \in \mathbb{N}, 1 \leq c \leq \dim(\mathcal{X}_1)\}$. The covariance matrix can either be a standard covariance matrix with a full set of entries or can be an approximation with entries only on the diagonal of the matrix, i.e., we define $\mathbf{\Sigma} = \{\text{“full”}, \text{“diagonal”}\}$. The reason behind the choice of both types of covariance matrix is also motivated by heuristical optimization. The full covariance matrix can result in overfitting, especially on small datasets, whereas the diagonal matrix acts as a type of regularization to the model. However, depending on the data the diagonal type sometimes also leads to an underfitting of the model.

After fitting a GMM on $\mathcal{X}'_1$ the first metric for the selection is calculated. Precisely, the bayesian information criterion (BIC) is calculated as in Equation **??** (see Section **??**). Note, that for the case of a diagonal covariance matrix, the number of entries of the covariance matrix to estimate changes from $\frac{D(D+1)}{2}$ to $D$. Thus, given a GMM with $K$ mixture components, each exhibiting a diagonal covariance matrix, and a datasset $\mathcal{X}_1$ consisting of $N$ data points and $D$ features, the BIC is defined as

$$\text{BIC}(\text{GMM}|\mathcal{X}_1) = (KD + D + K - 1)\ln(N) - 2\ln(\hat{L}). \tag{4.2}$$

After that, a second evaluation metric is calculated (see Algorithm 8). The process that is used to gather that metric is called adversary evaluation and is based on the principles of Generative Adversarial Networks (GANs).

```
Input: Dataset $\mathcal{X}_1$
Output: Tuple ($GMS$, GMM, PCA)
$\mathcal{X}'_1 \leftarrow \text{PCA}(\mathcal{X}_1)$
$\mathcal{C} \leftarrow \{4c \,|\, c \in \mathbb{N}, 1 \leq c \leq \dim(\mathcal{X}_1)\}$
$\mathbf{\Sigma} \leftarrow \{\text{“full”}, \text{“diagonal”}\}$
$L \leftarrow$ new list
for each $c$ in $\mathcal{C}$ do
    for each $\Sigma$ in $\mathbf{\Sigma}$ do
        $\text{GMM} \leftarrow \text{fitGaussianMixture}(\mathcal{X}'_1, c, \Sigma)$
        $\text{BIC} \leftarrow \text{BIC}(\text{GMM}, \mathcal{X}'_1)$
        $ACC \leftarrow \text{AdversaryEvaluation}(\mathcal{X}_1, \text{GMM}, \text{PCA})$
        $GMS \leftarrow GMS(\text{BIC}, ACC)$
        add ($GMS$, GMM, PCA) to $L$
sort $L$ according to the values of $GMS$
return ($GMS$, GMM, PCA) with the lowest value for $GMS$
```

Algorithm 7: Model Selection

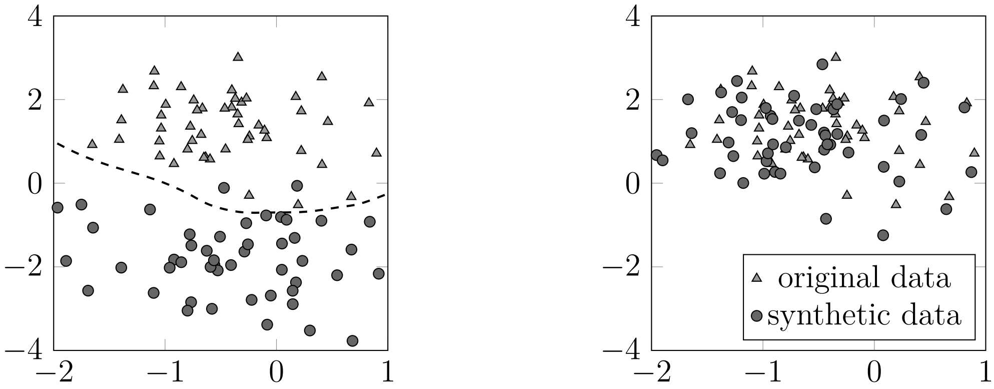

(a) A poor fitted generative model: The original data (triangles) and the synthetic data (circles) can be easily separated by a classifier.

(b) A well fitted generative model: The synthetic data resemble the original data well, such that a separation is not easy.

Figure 4.7: Adversary evaluation: seperate original and fake data.

Fitting a Generative Adversarial Network (GAN) involves a discriminator function, i.e., classifier that tries to distinguish between the original and synthetic data. In other words, the generative algorithm synthesizes fake data, which resembles the original data. Based on that, a dataset is assembled by combining fake data labeled as the positive class (1) and original data labeled as the negative class (0) or vice versa. This dataset is shuffled and split into a training and test proportion.

Then, a discriminative model is trained on the training proportion, trying to find distinguishing features within both classes, allowing a distinction to be made. Within the evaluation step, the discriminator is tested on its ability to separate fake and original data. The lower the score of the discriminator, the better the generative model. Figure 4.7 illustrates two scenarios. In the first scenario (a), the generative model has been fitted poorly, because the synthetic data can be easily separated from the original data as indicated by the decision boundary (dashed line). In the second scenario (a), the generative model performs well by creating synthetic data that could not be seperated from the original data.

```
**Input:** $\mathcal{X}_1, \mathrm{GMM}, \mathrm{PCA}$
**Output:** $ACC$ from decision tree model $DT$
$\tilde{\mathcal{X}}_1' \leftarrow$ sample $|\mathcal{X}_1|$ data points from GMM
$\tilde{\mathcal{X}}_1 \leftarrow \mathrm{PCA}^{-1}(\tilde{\mathcal{X}}_1')$
$\mathcal{Y} \leftarrow \{1\}$
$\tilde{\mathcal{Y}} \leftarrow \{0\}$
$\mathcal{D} \leftarrow \mathrm{concatenate}(\mathcal{X}_1 \times \mathcal{Y}, \tilde{\mathcal{X}}_1 \times \tilde{\mathcal{Y}})$
$\mathcal{D}_{\mathrm{train}}, \mathcal{D}_{\mathrm{test}} \leftarrow \mathrm{shuffleSplit}(\mathcal{D})$
$\mathrm{DT} \leftarrow \mathrm{fitDecisionTree}(\mathcal{D}_{\mathrm{train}})$
$\hat{\mathcal{Y}} \leftarrow$ predict $\mathcal{X}_{\mathrm{test}} \subset \mathcal{D}_{\mathrm{test}}$ with DT
$ACC \leftarrow ACC(\mathcal{Y}_{\mathrm{test}}, \hat{\mathcal{Y}})$
**return** $ACC$
```

Algorithm 8: Adversary Evaluation

In order to quantify the performance of the discriminator within the adversary evaluation, a classification metric is calculated. Since the original and synthetic data is equal in size and the posed problem is binary the $ACC$ is chosen, which is defined as

$$ACC = \frac{TP + TN}{TP + TN + FP + FN} \tag{4.3}$$

For each iteration in the model selection process, both the BIC and the $ACC$ are stored. After all parameter combinations have been exhausted and all resulting models have been evaluated a combined metric is calculated from the BIC and $ACC$ for each model. For that, the value range of both metrics must be aligned, such that the BIC is normalized into the range $[0, 1]$ by applying the min-max-normalization from Equation 4.1. After that, the mean is calculated for each metric pair as defined in Equation 4.4. Finally, the model with the lowest combined metric $m$ is selected.

$$GMS = \frac{1 - ACC + \text{BIC}}{2}. \tag{4.4}$$

The model parameters of both the GMM and the PCA are stored in the $PDB_G$. In numbers, these can range, depending on which type of covariance matrix is chosen for the GMM. PCA on the other hand, requires a $D \times M$ projection matrix, with $D$ being the dimensions of the original data space and $M$ being the number of dimensions in the projected subspace. Note that $|\mathcal{S}_y|$ defines the number of unique labels within a region, which effectively determines the number of model pairs (GMM, PCA) that are to be stored per region. Therefore, per region, the number of parameters to store is at least

$$|\mathcal{S}_y| \, (2KD + K - 1 + MD)$$

and at most

$$|\mathcal{S}_y| \, \Big((KD + K \, \frac{D(D+1)}{2} + K - 1) + MD\Big).$$

### 4.3.4 Classifier Fitting

The objective of the classifier fitting service is to provide the local IDS with the latest classification model trained on both original local data and synthetic global data. After each change to the generative models in the global pattern database made by the previous service, an event is sent into the communication channel. Within a defined time window, all such events are collected. If at least a single event was collected, the classifier fitting service is initiated and begins with assembling a training dataset. For this task, all original data are first loaded from the local PDB. Then, all generative models are loaded sequentially from the PDB and provided. n the process, synthetic data is generated in the amount that was also originally found in the corresponding region. After each sampling, the synthetic data is transferred from the lower-dimensional subspace to the original data space by the inverse function of the original PCA operation. Subsequently, the normalization operation is also reversed for both the original and the synthetic data by loading the corresponding parameters that were used to normalize a batch from the PDB.

**Input:** Region Update Event $r$
**Output:** Model Update Notification

Algorithm 9: Dataset Assembly and Classifier Fitting

## 4.4 Summary

# Chapter 5

# Experimental Evaluation

## 5.1 Flow Feature Analysis

### 5.1.1 Datasets

### 5.1.2 Feature Extraction and Preprocessing

## 5.2 Experimental Setup

### 5.2.1 Implementation Details

### 5.2.2 Methodologies

## 5.3 Evaluation Results

### 5.3.1 Classification Improvement

### 5.3.2 Overhead Reduction

## 5.4 Summary and Discussion

# Chapter 6

# Conclusion and Outlook

## 6.1 Conclusion

## 6.2 Outlook

# Bibliography

[Den87] Dorothy E Denning. "An intrusion-detection model". In: *IEEE Transactions on software engineering* 2 (1987), pp. 222–232.

[Cla88] David Clark. "The design philosophy of the DARPA Internet protocols". In: *Symposium proceedings on Communications architectures and protocols*. 1988, pp. 106–114.

[Seb+88] Michael M Sebring et al. "Expert systems in intrusion detection: A case study". In: *Proceedings of the 11th National Computer Security Conference*. 1988, pp. 74–81.

[LTG92] Teresa F Lunt, Ann Tamaru, and F Gillham. *A real-time intrusion-detection expert system (IDES)*. SRI International. Computer Science Laboratory, 1992.

[IM98] Piotr Indyk and Rajeev Motwani. "Approximate nearest neighbors: towards removing the curse of dimensionality". In: *ACM Symposium on Theory of Computing* (1998).

[VK98] Giovanni Vigna and Richard A Kemmerer. "NetSTAT: A network-based intrusion detection approach". In: *Proceedings 14th Annual Computer Security Applications Conference (Cat. No. 98EX217)*. IEEE. 1998, pp. 25–34.

[Ken99] Kristopher Kristopher Robert Kendall. "A database of computer attacks for the evaluation of intrusion detection systems". PhD thesis. Massachusetts Institute of Technology, 1999.

[Roe+99] Martin Roesch et al. "Snort: Lightweight intrusion detection for networks." In: *Lisa*. Vol. 99. 1. 1999, pp. 229–238.

[VK99] Giovanni Vigna and Richard A Kemmerer. "NetSTAT: A network-based intrusion detection system". In: *Journal of computer security* 7.1 (1999), pp. 37–71.

[Axe00] Stefan Axelsson. "The base-rate fallacy and the difficulty of intrusion detection". In: *ACM Transactions on Information and System Security (TISSEC)* 3.3 (2000), pp. 186–205.

[Cha02] Moses S Charikar. "Similarity estimation techniques from rounding algorithms". In: *Proceedings of the thiry-fourth annual ACM symposium on Theory of computing*. 2002, pp. 380–388.

[Cla04] Benoît Claise. *Cisco Systems NetFlow Services Export Version 9*. https://rfc-editor.org/rfc/rfc3954.txt. Accessed: 2021-03-11. 2004.

[WS04] Ke Wang and Salvatore J Stolfo. "Anomalous payload-based network intrusion detection". In: *International workshop on recent advances in intrusion detection*. Springer. 2004, pp. 203–222.

[Dep+05] Ozgur Depren et al. "An intelligent intrusion detection system (IDS) for anomaly and misuse detection in computer networks". In: *Expert Systems with Applications* 29.4 (2005), pp. 713–722. ISSN: 0957-4174. DOI: https://doi.org/10.1016/j.eswa.2005.05.002. URL: https://www.sciencedirect.com/science/article/pii/S0957417405000989.

[Sav05] Stefan Savage. "Internet outbreaks: epidemiology and defenses". In: *Invited Talk in the 12th Annual Network and Distributed System Security (NDSS 05)*. 2005.

[Szo05] Peter Szor. *The Art of Computer Virus Research and Defense: ART COMP VIRUS RES DEFENSE _p1*. Pearson Education, 2005.

[AI06] Alexandr Andoni and Piotr Indyk. "Near-optimal hashing algorithms for approximate nearest neighbor in high dimensions". In: *2006 47th annual IEEE symposium on foundations of computer science (FOCS'06)*. IEEE. 2006, pp. 459–468.

[Bis06] Christopher M. Bishop. *Pattern recognition and machine learning*. Springer, 2006.

[MNP06] Rajeev Motwani, Assaf Naor, and Rina Panigrahi. "Lower bounds on locality sensitive hashing". In: *Proceedings of the twenty-second annual symposium on Computational geometry*. 2006, pp. 154–157.

[ZZ06] Jiong Zhang and Mohammad Zulkernine. "A hybrid network intrusion detection technique using random forests". In: *First International Conference on Availability, Reliability and Security (ARES'06)*. IEEE. 2006, 8–pp.

[Cla08] Benoît Claise. *Specification of the IP Flow Information Export (IPFIX) Protocol for the Exchange of IP Traffic Flow Information*. https://rfc-editor.org/rfc/rfc5101.txt. Accessed: 2021-03-11. 2008.

[McK+08] Nick McKeown et al. "OpenFlow: Enabling innovation in campus networks". In: *Computer Communication Review* (2008).

[ZLK10] Chenfeng Vincent Zhou, Christopher Leckie, and Shanika Karunasekera. "A survey of coordinated attacks and collaborative intrusion detection". In: *Computers & Security* 29.1 (2010), pp. 124–140.

[TB11] Brian Trammell and Elisa Boschi. "An introduction to IP flow information export (IPFIX)". In: *IEEE Communications Magazine* 49.4 (2011), pp. 89–95.

[RGH12] Damien Riquet, Gilles Grimaud, and Michaël Hauspie. "Large-scale coordinated attacks: Impact on the cloud security". In: *2012 Sixth International Conference on Innovative Mobile and Internet Services in Ubiquitous Computing*. IEEE. 2012, pp. 558–563.

[Hof+14] Rick Hofstede et al. "Flow Monitoring Explained: From Packet Capture to Data Analysis With NetFlow and IPFIX". In: *Communications Surveys & Tutorials, IEEE* (2014).

[LRU14] Jure Leskovec, Anand Rajaraman, and Jeffrey David Ullman. "Finding Similar Items". In: *Mining of Massive Datasets*. 2nd ed. Cambridge University Press, 2014, pp. 68–122. DOI: 10.1017/CBO9781139924801.004.

[Mil+15] Aleksandar Milenkoski et al. "Evaluating computer intrusion detection systems: A survey of common practices". In: *ACM Computing Surveys (CSUR)* 48.1 (2015), pp. 1–41.

[Vas16] Emmanouil Vasilomanolakis. “On Collaborative Intrusion Detection”. PhD thesis. Darmstadt: Technische Universität Darmstadt, 2016. URL: http://tubiblio.ulb.tu-darmstadt.de/82583/.

[Rub18] Aviad Rubinstein. “Hardness of approximate nearest neighbor search”. In: *Proceedings of the 50th annual ACM SIGACT symposium on theory of computing*. 2018, pp. 1260–1268.

[WM18] Michael E. Whitman and Herbert J. Mattord. *Principles of information security*. Cengage Learning, 2018. ISBN: 978-1-337-10206-3.

[DFO20] Marc Peter Deisenroth, A. Aldo Faisal, and Cheng Soon Ong. *Mathematics for machine learning*. Cambridge University Press, 2020.

[Hin+20] Hanan Hindy et al. “A taxonomy of network threats and the effect of current datasets on intrusion detection systems”. In: *IEEE Access* 8 (2020), pp. 104650–104675.

[Bee21] Frank Beer. “A Hybrid Flow-based Intrusion Detection System Incorporating Uncertainty”. PhD thesis. University of Kassel, 2021.

[NBJ21] Parth Nagarkar, Arnab Bhattacharya, and Omid Jafari. “Exploring State-of-the-Art Nearest Neighbor (NN) Search Techniques”. In: *8th ACM IKDD CODS and 26th COMAD*. 2021, pp. 443–446.

[TFW21] A.S. Tanenbaum, N. Feamster, and D.J. Wetherall. *Computer Networks, Global Edition*. Pearson Education, 2021. ISBN: 9781292374017. URL: https://books.google.de/books?id=nT4QEAAAQBAJ.

[Pha] Peter Phaal. *sFlow Specification Version 5*. https://sflow.org/sflow_version_5.txt. Accessed: 2022-08-10.

[Wil] S. William. *Cryptography and Network Security - Principles and Practice, 7th Edition*. Pearson Education India. ISBN: 9789353942564. URL: https://books.google.de/books?id=AhDCDwAAQBAJ.

# List of Abbreviations

| | |
|---|---|
| $ACC$ | accuracy score |
| $GMS$ | generative model selection |
| $c$-ANN | $c$-approximate nearest-neighbour problem |
| $cr$-ANN | $cr$-approximate nearest-neighbour problem |
| BIC | bayesian information criterion |
| CIDS | Collaborative Intrusion Detection System |
| CIDSM | Collaborative Intrusion Detection System Message |
| DGM | Deep Generative Models |
| DoS | Denial of Service |
| DPI | Deep Packet Inspection |
| DR | Detection Rate |
| EM Algorithm | Expectation Maximization Algorithm |
| FPF | Flow Processing Format |
| FPR | False Postive Rate |
| GAN | Generative Adversarial Network |
| GMM | Gaussian Mixture Model |
| GRP | gaussian random projection |
| HIDS | Host-based Intrusion Detection System |
| IDS | Intrusion Detection System |
| LSH | locality-sensitive hashing |
| LVM | Latent Variable Model |
| MLE | Maximum Likelihood Estimation |
| NIDS | Network-based Intrusion Detection System |
| NN | nearest-neighbour search problem |
| ONB | Orthonormal Basis |
| PCA | Principal Component Analysis |
| QoS | Quality of Service |
| R2L | Remote to Local |
| U2R | User to Root |

# List of Symbols

### General Mathematical Notation

| | |
|---|---|
| $\mathbb{N}$ | natural numbers |
| $\mathbb{R}$ | real numbers |
| $\mathbb{R}^n$ | $n$-dimensional vector space of real numbers |
| $a, b, c$ | scalars are lowercase |
| $\boldsymbol{x}, \boldsymbol{y}, \boldsymbol{z}$ | vectors are bold lowercase |
| $\boldsymbol{A}, \boldsymbol{B}, \boldsymbol{C}$ | matrices are bold uppercase |
| $\mathcal{A}, \mathcal{B}, \mathcal{C}$ | sets |
| $\boldsymbol{x}^\top, \boldsymbol{A}^\top$ | transpose of a vector or matrix |
| $\boldsymbol{A}^{-1}$ | inverse of a matrix |
| $\boldsymbol{x}^\top \boldsymbol{y}$ | dot product of $\boldsymbol{x}$ and $\boldsymbol{y}$ |
| $B = (\boldsymbol{b_1}, \boldsymbol{b_2}, \boldsymbol{b_3})$ | (ordered) tuple |
| $\boldsymbol{B} = [\boldsymbol{b_1}, \boldsymbol{b_2}, \boldsymbol{b_3}]$ | matrix of column vectors stacked horizontally |
| $\mathcal{B} = \{\boldsymbol{b_1}, \boldsymbol{b_2}, \boldsymbol{b_3}\}$ | set of vectors |
| $a \in \mathcal{A}$ | $a$ is element of the set $\mathcal{A}$ |
| $a \notin \mathcal{A}$ | $a$ is not element of the set $\mathcal{A}$ |
| $\{a \in \mathcal{A} \mid \phi\}$ | set containing all $a \in \mathcal{A}$ meeting condition $\phi$ |
| $\lvert\mathcal{A}\rvert$ | cardinality of the set $\mathcal{A}$ |
| $a \gg b$ | $a$ is much greater than $b$ |

### Architecture Specification

| | |
|---|---|
| $N \in \mathbb{N}$ | number of data points; indexed by $n = 1, \dots, N$ |
| $D \in \mathbb{N}$ | number of dimensions; indexed by $d = 1, \dots, D$ |
| $M \in \mathbb{N}$ | number of members in the CIDS; indexed by $m = 1, \dots, M$ |
| $\mathcal{X}$ | input space |

| | |
|---|---|
| $\mathcal{Y}$ | space of true targets, i.e., classes |
| $\mathcal{D}$ | training dataset |

# List of Tables

# List of Figures

# List of Algorithms